

FINAL PUBLISHABLE JRP REPORT

JRP-Contract number	IND13	
JRP short name	T3D	
JRP full title	Thermal Design and Time-Dependent Dimensional Drift Behaviour of Sensors, Materials and Structures	
Version numbers of latest contracted Annex Ia and Annex Ib against which the assessment will be made	Annex Ia:	V1.0
	Annex Ib:	V1.0
Period covered (dates)	From 01 October 2011	to 30 September 2014
JRP-Coordinator		
Name, title, organisation	Dr. Jens Flügge, PTB	
Tel:	+49 531 592 5200	
Email:	Jens.Fluegge@ptb.de	
JRP website address	projects.npl.co.uk/T3D/	
Other JRP-Partners		
Short name, country	PTB, Germany	
	LNE, France	
	NPL, United Kingdom	
	VSL, Netherlands	
	ENSMA, France	
	FhG, Germany	
REG1 – Researcher (associated Home Organisation)	Dr. Marc Schalles TU Ilmenau, Germany	Start date: 01 Oct 2011 Duration: 36 months

Report Status: PU Public



TABLE OF CONTENTS

1	Executive Summary	3
2	Project context, rationale and objectives.....	4
3	Research results	7
4	Actual and potential impact.....	38
5	Website address and contact details	43
6	List of publications.....	43

1 Executive Summary

Introduction

This project developed approaches for measuring small changes in the accuracy of sensors, and in the dimensions and properties of materials and structures, used in precision engineering. The project developed new measurement equipment, facilities, modelling approaches, and standardised procedures, which will be used by a range of European industries to enhance their precision engineering capabilities to develop higher-performance, internationally competitive products.

The Problem

Precision engineering is central to maintaining and promoting the international competitiveness of European companies in a range of industries, including electronics, aerospace, semiconductors, and nano-materials. These industries rely on ultra-precision production techniques and sophisticated measurement instruments to develop ever smaller and higher-performance products.

However, such fine levels of precision are vulnerable to even small changes in the dimensions and properties of sensors, materials and production equipment, reducing the levels of accuracy and precision that can be achieved. Such changes occur through time, and can be caused by temperature fluctuations in the production environment, and mean that precision engineering equipment requires regular re-calibration, halting production, and that it must often be maintained in costly temperature-controlled laboratories.

The production efficiency and international competitiveness of a range of European industries will be enhanced through the development of more stable and temperature-resistant materials and measurement devices, supporting the development of increasingly stable precision engineering equipment.

Impact

Dissemination of results

To promote the uptake of the project's results, outputs were shared broadly with scientific and industrial end-users. 20 papers have, or are in the process, of being published in international journals, 34 presentations have been made at national and international conferences, and three presentations at exhibitions. Two workshops on the project were held during the 2014 European Society for Precision Engineering and Nanotechnology conference in Dubrovnik, and the 2014 IWK conference in Ilmenau. Results have been shared with stakeholder companies, and standards committees governing hardness and nano-measurement science, through 11 in-house workshops. Measurement data from the testing of material and joint samples has been made available through a public database, and experience and results have been described in good practice guides and 26 publications available on the project website and the [EURAMET Publications Repository](#).

Early impact

The project's results are allowing precision instrument manufacturers to further improve the performance and stability of their products.

For instance, the [Fraunhofer IOF](#) research institute, an unfunded research partner, needed methods to measure the time and temperature dependent properties of their products. Fraunhofer IOF have developed and refined specialized inorganic joining techniques, including silicate bonding, Au/Sn laser-based thin-film soldering, and Solderjet Bumping, to assemble optical components for ultra-high-precision instruments. Fraunhofer IOF produced sample materials for the project, which were assessed for time scales of over one year, and for temperatures between 10 °C and 40 °C. The results of this testing have provided Fraunhofer IOF with a detailed assessment of these joining techniques, and have allowed them to guarantee the stability of their joining techniques to their customers.

A prototype room-temperature measurement system was developed for objective 4, and is now available to precision engineering tool manufacturers. The system can be used to assess the effects of temperature on their products, and to help develop more thermally-stable instruments. For example, [SIOS Meßtechnik GmbH](#), a manufacturer of precision laser-interferometric measuring instruments, used the prototype system to monitor temperature changes at their facility and to understand their instruments' thermal stability. Using

this data, they have improved an ultra-precise dimensional measurement instrument by eliminating small uncertainties related to temperature fluctuations. The product will allow their customers to measure small components such as microelectronic, micromechanical or optical objects, to sub-nanometre precision, without the need for highly controlled environments.

During the development of the prototype temperature measurement system, the project team commissioned instrument manufacturer [Magnicon GmbH](#) to develop a high-sensitivity SQUID amplifier suitable for room-temperature measurements. SQUID amplifiers are used to amplify very small changes in voltage to levels that can be measured with a high degree of accuracy, therefore were judged to be suitable amplifiers for the prototype system, which measured temperature changes in terms of voltage changes (via thermocouples). However, before the project, there were no commercially available SQUIDs suited to room-temperature measurement. Through contributing to the project, Magnicon developed a room-temperature SQUID amplifier, a completely new application for their technology, and have since launched new room-temperature products.

The project also commissioned [MPro GmbH](#), a developer of custom electronics, to contribute to the development of the room-temperature measurement system. Since project completion, MPro have begun to develop a commercial version of the system to be launched in 2017, expanding MPro's product line and making the project's prototype more widely available to other National Measurement Institutes, research facilities and manufacturers.

[MicroMaterials](#), a leading manufacturer of nanomechanical test instruments, has also adopted procedures developed in the project as alternative techniques for monitoring and controlling specimen and indenter temperatures for their instruments.

Early impact will also be achieved through the development of new and improved calibration services for the measurement of thermal dilatation and dimensional stability for material samples, and for joints, sensors and actuators. Additionally, NPL is now able to perform indentation measurements for a greater temperature range, LNE can now provide industrial customers with more accurate thermally optimised cylindricity comparator measurements, and PTB can offer sample preparation (for secondary calibration), particularly for smaller companies.

Potential future impact

The knowledge, techniques and instruments developed in this project are available to European industry, and will allow end-users to accurately measure and manage thermal and time-dependent drift in their precision engineering processes, and to develop more time and temperature-stable precision engineering equipment. These developments will reduce time, energy consumption and costs in manufacturing, and will ultimately support the development of higher-performance, internationally-competitive products.

2 Project context, rationale and objectives

With current trends in precision engineering towards ever-higher accuracies for industrial high-end production and measurement equipment, especially from ICT or aerospace industries, temperature effects and time-dependent drift become a serious limitation for achievable system performance. Nearly all high precision measurement and production tools (including tool machines, photolithography tools, high resolution microscopes, balances, electrical measurement equipment and various other instruments) are affected and performance-limited by variations in environmental parameters like temperature, humidity, air pressure, and temporal stability of the adjustment of instrument components.

The "Roadmap Precisetehnologie" [1] stated a need for detailed knowledge of the stability of materials, joints and sensors on medium-term (hours to weeks) to long-term (a year) timescales, and also knowledge of thermal parameters of these components for an improved tool design and to assure efficient and economic use of the tools. Strategic documents [2,3] have emphasised a need for accurate measurement of thermal influences, in order to optimise manufacturing and measurement processes in many areas including: optics and semiconductor manufacturing, precision tool machines, aerospace applications, climate control. While new materials are increasingly used, there are open issues in the metrology framework for reference materials and related standardisation. Furthermore, mandates for the development of indentation-based



methods exist from the ISO/TC 164/SC2 and SC3 committees for ductility and hardness testing, respectively [4].

The highest requirements in precision today exist in the semiconductor device manufacturing. Therefore the focus of the project is mainly to generate tools and knowledge for this industry branch. The development of the needs is well documented in the ITRS roadmap [5], where it is clearly stated, that thermal dilatation with uncertainties of 10^{-10} and drift measurement in the range of 0.1 nm and even below are a key to further miniaturisation.

These limitations can be overcome by a more insensitive design of machine components which requires an improved knowledge of material and joint properties and by active compensation of thermal gradients caused by heat sources or drains since tool stability directly correlates with the system performance/ process control, and can be improved by better environmental control or by a more insensitive design. Additionally, progress in the knowledge about thermal behaviour and stability of materials and joints as well as guidance for thermal modelling will also allow design of more economical machines with lower precision demands and relaxed environmental conditions to minimize energy consumption.

To minimise the sensitivity regarding time and environmental conditions of machine tool design different methods can be used. It can be done by choosing more stable materials and joining technologies, by measuring of dimensional changes using additional sensors, which have to be drift and temperature insensitive themselves or by active control of a heat flow in the machine. For highest accuracy all of these methods have to be combined. In all cases it is necessary to have exact information on the properties of materials, machine components such as frames, mounting elements and sensors. So far there have been no comparisons between the measurement results from different type of dimensional measurement instruments; therefore the project will develop a calibration standard to validate and calibrate the instruments for dilatation, aging, and surface behaviours such as hardness and creep.

A key for the design of thermally optimizing machine tools is nowadays the thermal modelling. Due to high calculation times FEM methods are too slow to incorporate the calculations in model based control algorithms, reduced models have to be used, which must be verified. Temperature control naturally also requires appropriate temperature measurement equipment, which also allows for the verification of thermal modelling. Beside accuracy in the millikelvin range or even below, it is especially important to find economical solutions with low maintenance time and costs to allow for a widespread use in industry.

The work done in this project involved different techniques to improve precision engineering tools regarding environmental and time dependent influences. The work program has been discussed with the stakeholders and has been complemented by their needs. Some of the stakeholders supplied the project with samples of different joining technologies and new materials, which ensured the relevance of the measurements for industrial applications. Others helped with the test of the equipment under industrial conditions.

Many organisations have investigated the stability and thermal behaviour of precision machines, both for in house development and also to contribute to the large body of scientific publications. However, the fast pace in increasing accuracy requirements underpins an ongoing need. The following table shows the current state of the art:

Measurement technique	Current state of the art
Highest precision dimensional measurement machines e.g. <ul style="list-style-type: none"> - wafer scanners (ASML, Nikon), - mask metrology systems (Zeiss, KLA-Tencor) - diamond turning machines 	Positional reproducibility of ~ 1 nm, over medium time frames (including performance of the sensor systems, stability of the measurement frame and the sensor mounting) target: 10 pm or better uncertainty over days/weeks
Interferometry measurement equipment	0.5 nm uncertainty, for samples up to 50 mm over years (long term) Used for: measurement of drift, thermal expansion and compressibility

	target: 10 pm or better uncertainty over days/weeks
Fabry-Pérot displacement interferometer in the lab with complex sample preparation required	10 pm uncertainty with samples up to 50 mm for minutes duration (short term) target: 10 pm or better uncertainty over days/weeks
Temperature measurement systems: using pair of annually calibrated resistance thermometers	0.5 mK reproducibility with annual calibration required (unacceptable down time) Used for: verification of thermal modelling, measurement of sample temperatures and thermal control loops in machines Target: low maintenance thermocouples for measurement of small temperature differences with reproducibility below 0.5 mK over more than a month. Temperature measurement using platinum resistance thermometers with in situ calibration with a measurement uncertainty of a few mK.
Thermal modelling and control system	Target: improvement of the thermal sensitivity by a factor of 10 with regard to the active temperature control of heat sources
Creep or hardness measurement	Sparse data and standards are not yet established for higher temperatures Target: establish creep and indentation standards at elevated temperatures
Coefficient of thermal expansion (CTE)	Currently most samples measured over a large temperature range, giving errors around 20 °C particularly for low CTE materials. Little information about variation in CTE between samples, which can exceed 100% Target: CTE measurement at 20 °C. Database with information for CTE distribution on materials commonly used in precision engineering.
Thermal behaviour of connection methods or sensors	Only sparse information available, then limited to over 1 nm accuracy Target: Sub nanometre accuracy

The overall objective of the project was to support optimised thermal stability of ultra precision engineering measurement and production tools over timescales of weeks to months.

To achieve this, the project gathered precise knowledge of

- material and joint properties (aging, thermal dilatation, indentation creep),
- temperature sensors (thermocouples, self calibrating sensors with fixed points from alloys) and
- thermal modelling and control (development of thermally insensitive machine designs).

Building on existing information, the project participants developed new instruments and methods, and used these to measure various selected samples of joints and materials common in precision engineering. These data were used to populate a database that supports improved machine design.

We expect the results of the project to help raise the precision in manufacturing and measurement tools and will therefore help to improve the quality of products, as this will reduce the number of defective goods and wastage, savings in raw materials and reduced machine time per part are possible. Requirements for room temperature control can help to reduce the energy consumption of machines of lower accuracy. The project can also add a small puzzle part in the further miniaturization of semiconductor devices, which will make a reduction of energy consumption possible.

The key objectives were:

1. Development of optical interferometric measurement equipment for the determination of dimensional drift with a measurement uncertainty of 10 pm to 100 pm (dependent on the timescale from minutes to weeks) over sample lengths of 0.05 m and durations up to one week.
2. Development of an improved indentation method (with traceable calibration at elevated temperatures and a measurement uncertainty analysis) for the measurement of hardness and indentation creep of samples in the nanometre range at elevated temperatures. Investigations of the thermal dependence of hardness and creep of materials with uncertainties about 1 nm in the range Ambient to >100 °C, including establishment of corresponding design rules of materials and joints. Investigations of the thermal dependence of hardness and creep of materials with uncertainties about 1 nm in the range ambient to >100 °C, including establishment of corresponding design rules of materials and joints.
3. Measurement of time and temperature dependent behaviour of samples by optical interferometry with an uncertainty below 0.5 nm for measurement length up to 300 mm. The time scale of the measurements can be over a year and the temperature range allows measurements from 15 °C to 30 °C. The setup additionally allows measurement inhomogeneity of sample stability and dilatation.
4. Development of self-calibrating resistance temperature sensors by fixed points near 20 °C using alloys. To enable improved temperature measurement and control electronics in regard of sensor compatibility, control parameter determination and ease of use including a verification of long time stability of thermocouples.
5. Development of improved thermal modelling
6. Setup of a database for measurement results of the JRP with information on stability, thermal dilatation and hardness of material samples, joint structures, sensors and actors
7. Good Practice Guide for developing temperature insensitive precision engineering measurement and tool machines. This includes the selection of appropriate materials and joining technologies as well as the placement of unavoidable heat sources in the machine and of the selection of temperature sensors in precision engineering.

3 Research results

3.1. Objective 1: Development of optical interferometric measurement equipment for the determination of dimensional drift with a measurement uncertainty of 10 pm to 100 pm over sample lengths of 0.05 m and durations up to one week.

3.1.1. Introduction

Interferometric methods are necessary for highest precision measurement of the stability of materials and joints. At PTB an gauge block interferometer for some time has been used to measure stability and CTE of material samples with a measurement uncertainty down to 0.1 nm over years. As the interferometer is working in a vacuum chamber it allows for a large variation of the environmental parameters. The interferometer was already fully running at the start of the project and has been used to perform a larger number of measurements.

The demand for higher accuracy over shorter time frames of days was formulated by equipment manufacturers for semiconductor lithography. Therefore at VSL a new picodrift interferometer was built using heterodyne phase detection with interpolation accuracy below 10 pm. This work was supported by technology developed in PTB. As no vacuum chamber was used, main effort was necessary for generating a stable environment.

3.1.2. Development of the picodrift Instrumentation and verification of the measurement uncertainty

The Picodrift interferometer has been designed at VSL to characterise and quantify the temporal stability of materials and material connections with picometer uncertainty. To achieve such a challenging target, a highly symmetric balanced heterodyne interferometer has been developed in close collaboration with TU Delft and TNO. Initial tests performed at TNO, prior to the start of this project, showed that temperature and pressure fluctuations limited the performance to well above the desirable 10 picometer uncertainty. Essential modifications to the configuration, determined with support of the PTB, were applied to improve the symmetry between the individual interferometer paths, remove the non-linear measurement response, improve the phase measurement routine, and decrease the sensitivity to environmental parameters. The current configuration of the instrument is schematically represented in **Error! Reference source not found.**, a photograph and schematic representation of the interferometer is shown in **Error! Reference source not found.**

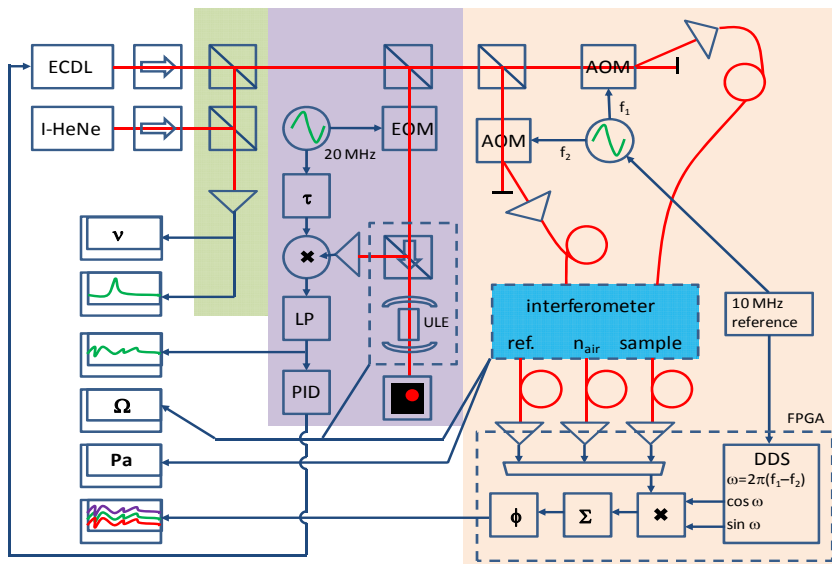


Figure 1: Schematic representation of the Picodrift instrument. The green block highlights the traceable detection of the laser oscillation frequency. The purple block along with the temperature and pressure sensors highlights the stabilisation and monitoring of external influences. The pink block highlights the beam preparation, beam delivery to the interferometer (blue block), signal detection, and data post-processing



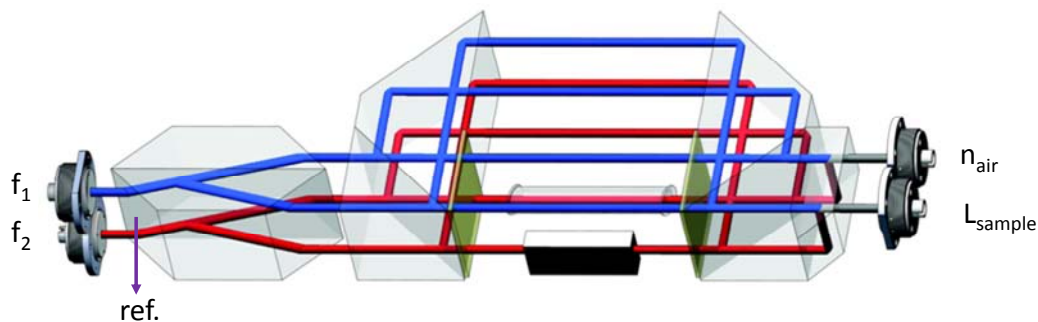


Figure 2. Picodrift interferometer (top) and schematic representation (bottom), with the laser beams delivered by the fiber couplers (left), split into two branches by the non-polarising beam-splitter, passing through two polarising beam-splitters equipped with a quarter wave-plate each, and recombined before being coupled into fibers (right) for signal detection and post-processing. One of the branches detects the length changes of the sample, while the other branch is used to measure the refractive index fluctuations and act as a reference.

The Picodrift instrument consists of a diode laser which is frequency locked to a stable ULE cavity using a Pound-Drever-Hall lock. The oscillation frequency is determined from a beat-note detection with a HeNe reference standard laser. The Allan deviation of the locked frequency results in a minimum deviation of less than 10 kHz between 1 to 45 s averaging time, corresponding to less than 2 pm uncertainty. The long term frequency drift is monitored using the beat-note measurements, and is typically of the order of 250 kHz per hour, and can be compensated for.

Subsequently, the laser beam is split into two paths with a frequency difference of 1.5 MHz between both beams. After polarisation clean-up, the beam is delivered to the interferometer which is placed inside a shielding box, shown in Figure 3. The temperature and pressure are monitored in the lab, and at various locations in the shielding box. After a period of acclimatisation, temperature gradients can be reduced to less than 0.5 mK per hour.

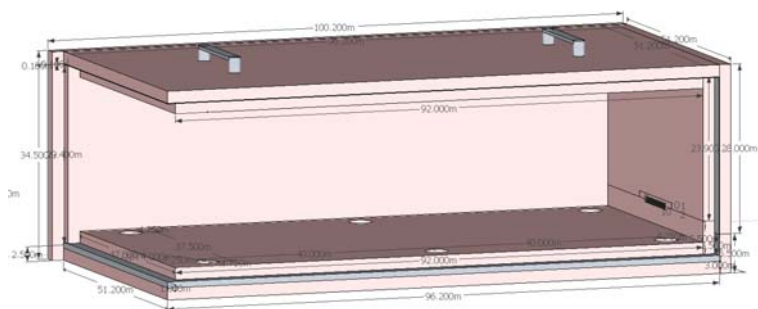


Figure 3. Shielding box used for temperature stabilisation. The temperature of the lab is controlled to be stable within 0.1 K. The box consists of two layers of styrofoam, with an aluminium layer in between for homogenisation. The box is covered by aluminium foil to reduce the effect of radiation.

The interferometer consists of two polarising beam-splitters equipped with a quarter wave-plate each, stress free placed on a highly stable base (stress relieved aluminium). In order to compensate for refractive index fluctuations, originating from the path length difference due to a non-zero sample length, an additional branch has been defined inside the interferometer. For reference, an third interference signal is available from reflection of the first surface of the non-polarising beam-splitter. The interference signal as detected by the low noise photo-receivers is filtered and amplified before being transferred to the 4 channel 120 MS/s analog-to-digital converter mounted on the fast FPGA-card. The FPGA is programmed using LabVIEW, and its clock frequency is indirectly locked to the split frequency of the laser beams. The FPGA demodulates the signal and converts the derived phase after averaging into a length change. The algorithm had been developed initially by PTB in a project of the iMERA+ program. An Allan deviation analysis has been performed, yielding a minimum deviation at a rate of 8 S/s. Since a slightly higher data rate is desirable, the

signals are averaged over 4,000,000 samples, or 50,000 periods, to arrive at a 30 S/s sample rate. The contribution of the electronic noise to the uncertainty in path length variations is of the order of 1 pm

The baseline performance of the interferometer has been determined using a double dead-path measurement where in both interferometer branches the sample and refractometer cell have been removed, respectively, as shown in Figure 4. The recorded temperature, pressure, and laser frequency change have been presented in Figure 5, and the refractive index fluctuations have been used for compensation of a 1.5 mm path length difference. The performance of the interferometer ranges from 5 pm for an 1 second interval, to 28 pm for an 1 hour interval.

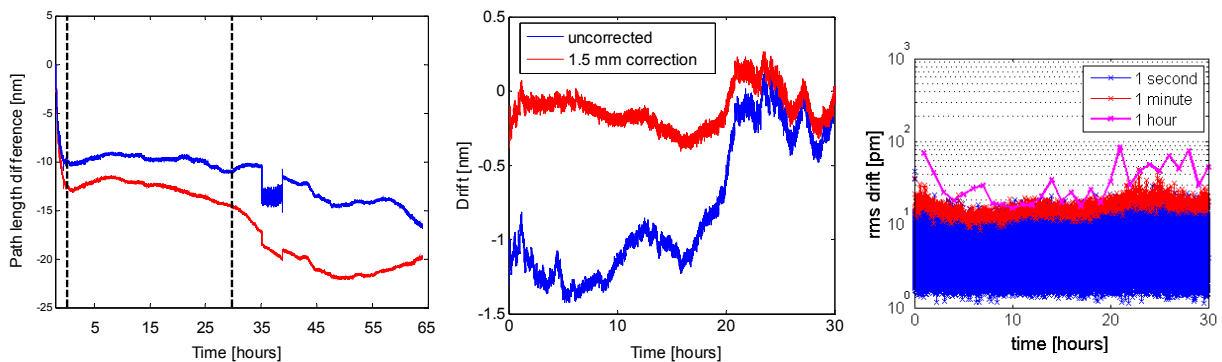


Figure 4. Double dead-path measurement for establishing the performance of the instrument. The path length change for the sample (blue) and refractometer (red) branch have been plotted as a function of time (left). The differential length change (center) between both branches (blue), and after compensation for a residual 1.5 mm path length difference (red), for a selected time-span. The root-mean-square of the differential path length plotted as a function of time for three different averaging intervals (right).

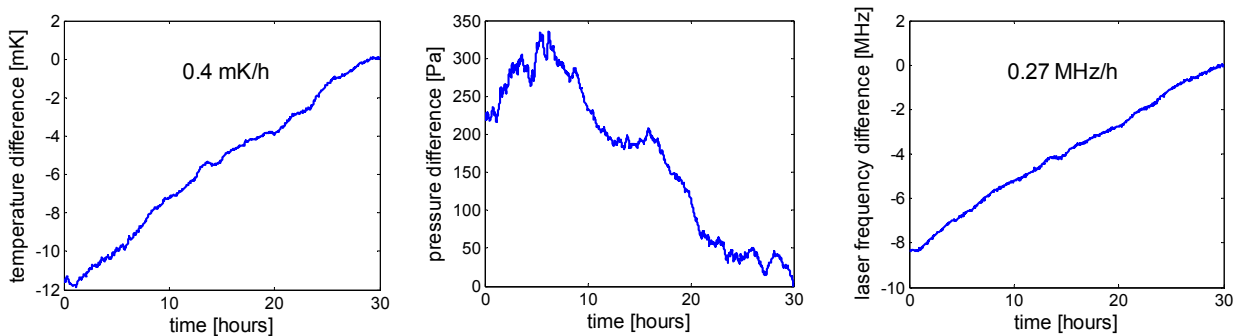


Figure 5. Recorded change of temperature (left), pressure (center), and laser frequency (right) as a function of time during the selected time-span as indicated in the figure above.

In general, the performance of the instrument is limited by any asymmetry between sample and reference interferometer, therefore it is essential to minimise or account for these asymmetries. As the alignment of the interferometer is never perfect, a sample measurement should always be preceded by a null-measurement of the empty interferometers to be able to account for the initial path length difference between both interferometers branches. Next, the refractometer interferometer should be matched to that of the sample interferometer with respect to optical path length and environment dependence. Afterwards, a period of acclimatisation is required to minimize temperature gradients, where the duration of this period is matched to the anticipated measurement duration, thermal properties of the sample, and correlation of environmental effects to the anticipated instability measurements. For longer durations of measurements, large pressure variations can influence the exact position of the beam-splitters, resulting in step-changes in the performance and required corrections of the interferometer, consequently a correlation of the monitored pressure and any observed effect should always be performed. Ultimately, it is essential to have an excellent polarisation purity, which can be enforced by adding additional polarisers in front of the detector, or even in the roundtrip arm, parallel to the sample and refractometer cell, of the interferometers.

The dimensions of the sample are relatively free to be chosen, but in case of use in the standard configuration should be at most 100 mm in length, and 40 mm in width and height. The sample should be mounted such that it can move freely, and is not affected by any strains or stresses. The end facets of the sample should be parallel (better than 3 arcmin) and reflective. The material properties should be known to allow for a correction of expansion or compression effects due to temperature and pressure. Also the nominal length of the sample should be known in order to be able to compensate for environmental changes. Finally, the environmental parameters of the sample should be monitored, especially in case temperature gradients are likely to be present. If the measurement object is actively controlled, any heat production should be minimised and an active temperature control can be considered.

If the presented considerations are taken into account, the instrument is able to measure displacements in the picometer range. For short term stability measurements (seconds) the limiting measurement rms noise is approximately 5 pm, while for medium term measurements (hours) with stable weather conditions, the limiting measurement rms noise is approximately 30 pm. Long term measurements (several days) usually show periods with significant influence of pressure variations on the length change measurements, which cannot be compensated for, and dominate the observed measurement results (well above 100 pm). For displacement measurements of actuated samples, the measurement resolution is well below the 5 pm.

To improve the long term measurement uncertainty, an alternative configuration of the interferometer has been designed, and presented in Figure 6. The design consists of a pressure sealed enclosure for the interferometer, while allowing samples to be placed in ambient air as well as the pressure sealed environment. It also introduces two more interferometer branches to provide an accurate reference signal, and allows for the two different sample measurements locations. One reference branch will pass through ambient air, acting as the refractometer, while the other remains in the pressure sealed environment providing a continuous dead-path reference, lifting the restriction on sample length. If the baseline performance of the alternative interferometer is below 2 pm, it is straight forward to switch from relative measurements to absolute measurements, by locking the diode laser to a neighbouring mode of the ULE cavity and therefore changing the wavelength sufficiently to determine the integer times half-wavelength contribution to the length measurements. Additionally, the alternative design of the interferometer presents straight forward means to perform bulk modulus measurements by control of the pressure, and in case of active temperature control of the enclosure, also allows for measurement of the thermal expansion coefficient (CTE).

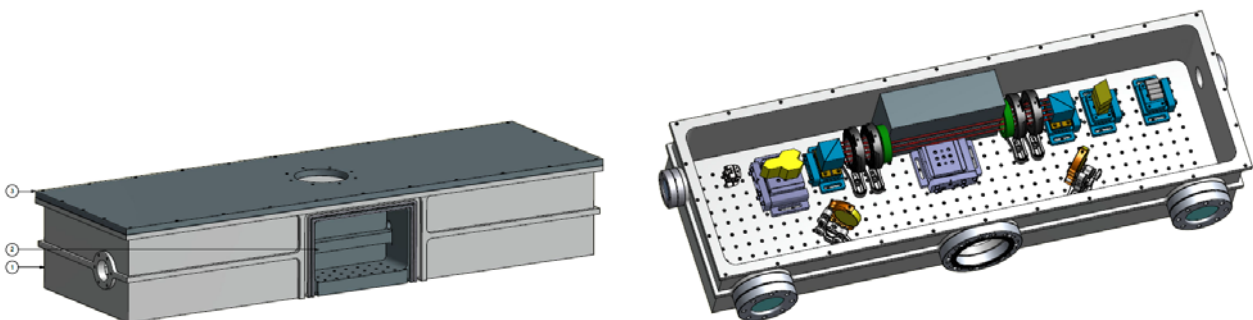


Figure 6. Pressure sealed enclosure of the interferometer (left), allowing for samples to be placed in ambient air as well as the pressure sealed environment. The interferometer includes two more interferometer branches to lift the stringent requirement on sample size by providing an accurate reference signal which includes the intrinsic interferometer drift in its signal, and to allow for dual sample measurements.

3.1.3. Conclusion and outlook

VSL, the Dutch NMI, developed an optical interferometer suitable for making picometre measurements of dimensional changes. Comparison measurements were performed against standard samples to calibrate measurements, and particular attention was paid to the temperature stability of the instrument. The baseline performance of the interferometer was determined using a double dead-path measurement, where both the sample and refractometer cell were removed and tested. The achievable uncertainties up to now depends on the stability of the weather conditions. The measurement uncertainty of the interferometer ranges from five picometres for one second intervals, and up to 28 picometres over an hour.

To achieve the objective by improving measurement uncertainties over longer time spans (from hours to weeks), a vacuum chamber for the interferometer was successfully designed and manufactured and will be in operation soon. This vacuum setup will also extend the measurement capabilities by allowing for bulk modulus measurements by control of the pressure in the chamber. An included temperature control of the vacuum chamber also improve the capability for determining the thermal expansion coefficient (CTE).

3.2. Objective 2: Development of an improved indentation method (with traceable calibration at elevated temperatures and a measurement uncertainty analysis) for the measurement of hardness and indentation creep of samples in the nanometre range at elevated temperatures.

3.2.1. Introduction

While optical measurement directly on the surface of the samples allow for the best possible accuracy, the effects to be measured are limited. A length change can be affected by internal structural changes when the material is not in thermodynamic equilibrium, e.g., after thermal treatment, but it is not possible to determine the effect of stress on the sample. Such investigations can be done by tactile probing using indenters. NPL has therefore characterized a new differential indenter instrument and added a heat shield to allow for measurements at elevated temperatures.

As there were no accepted procedures to calibrate the displacement of the high temperature nanoindentation equipment at elevated temperatures novel procedures had to be developed. Measuring the mechanical properties of specimens at elevated temperatures using nanoindentation requires accurate calibration of displacement, frame compliance and area function, as a function of temperature.

3.2.2. Novel methods for the calibration of indentation equipment at elevated temperatures

Until the new calibration procedures were developed, displacement “calibration” for the NanoTest was achieved by comparing the voltage output from the displacement capacitor plates to that of the x-y stage, as described in the manufacturer’s instructions. However, this was not an actual calibration as there was a lack of traceability to international standards. A procedure has therefore been developed to calibrate the displacement of the capacitor plates at elevated temperatures uses a Jamin interferometer, a schematic diagram of the apparatus used is shown in Figure 7.

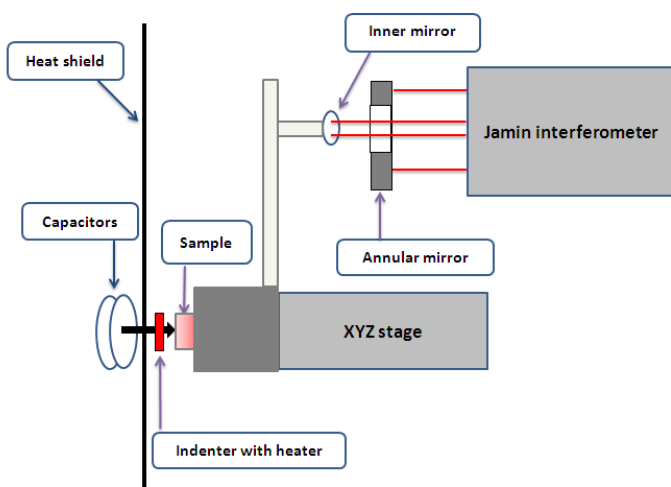


Figure 7: Schematic of the Nanotest indenter system with the Jamin optical interferometer setup for displacement calibration at high temperature.

Calibration of the area function at room temperature had previously been conducted by scanning the indenter tip using an AFM. Unfortunately, this technique was unsuitable for instruments operated at elevated temperatures as the geometry of the indenter tip could change significantly with temperature. Likewise the procedure previously used to determine the frame compliance could not be used at elevated temperatures as it involved removing the indenter tip from the instrument which is not possible using a high temperature hot-stage. An alternative method has therefore been developed to determine the area function and frame compliance using two well characterised reference materials. One material with a relative low stiffness used to obtain the area function and one material with a higher stiffness used to determine the frame compliance. A combination of freshly polished

Tungsten and fused Silica is recommended in ISO 14577. The use of tungsten at elevated temperature is, however, problematic as surface oxidation occurs at elevated temperatures. As instrumented indentation is

particularly sensitive to surface properties, this required substitute materials to be selected for elevated temperatures. Following an extensive literature search and testing using high temperature impact excitation two new reference have been selected which can be considered as a candidate reference material (CRM) for high temperature indentation.

With a robust calibration procedure developed an uncertainty budget was produced for the NPL Indentation Instrument that includes both instrument and environmentally derived uncertainties. The approach that was taken was to establish the uncertainty budget from the bottom up, based on the procedures for determining uncertainty in the “Guide to the Expression of Uncertainty in Measurement (GUM)”. One of the most important factors affecting the uncertainty budget was the effect that temperature had on the calibration of the instrument. Increasing the temperature at which the instrument was operated significantly altered both the calibration of the displacement and the load of the instrument (Figures 8 and 9) however interestingly for the for the NPL instrument it had little effect on either the frame compliance or the geometry of the indenter tip (Figures 10 and 11).

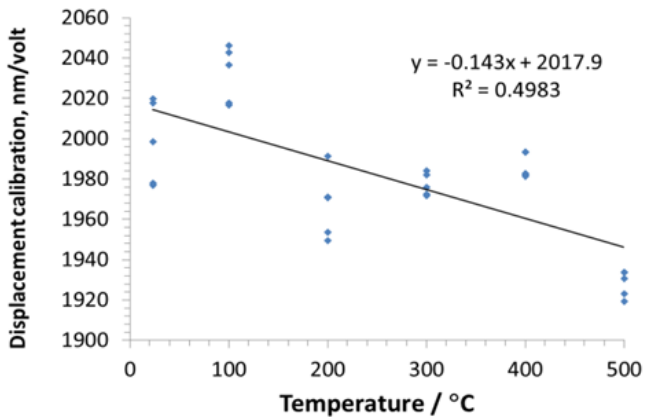


Figure 8: Load calibration as a function of temperature with two different experimental setups involving an open thermal shroud (red) and a closed shroud (blue). The open shroud increases the effect of the temperature on the force calibration.

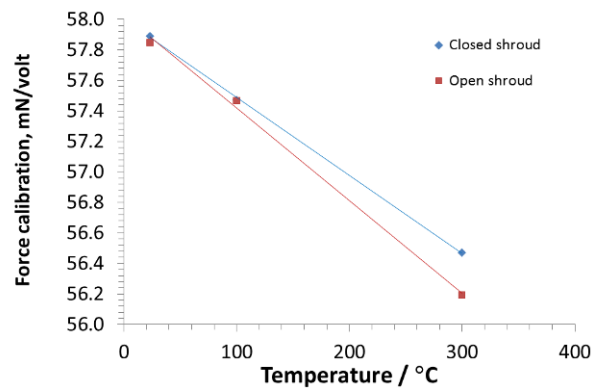


Figure 9: Influence of temperature on the displacement calibration of a nanoindentation

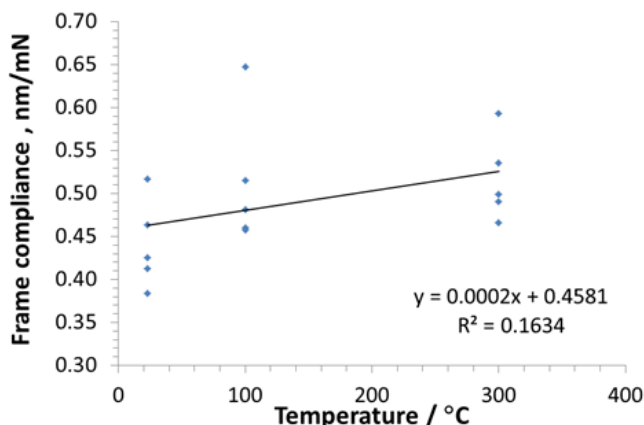


Figure 10: Frame compliance as a function of temperature from room temperature to 300°C.

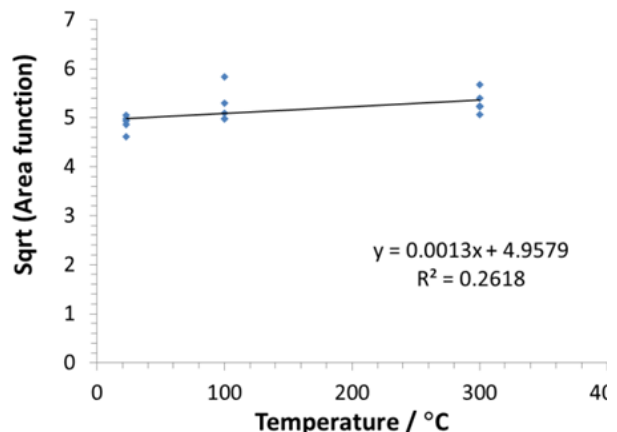


Figure 11: Area function as a function of temperature from room temperature to 300°C.

Another significant uncertainty in high temperature nanoindentation is in establishing the exact temperature of the specimen and the indenter. At elevated temperatures it is important to note that due to thermal gradients there is inevitably going to be a difference between the nominal temperature (i.e. the temperature set up on the temperature controllers) and the real temperature at the surface of the specimen beneath the

indenter. This is due to the location of the thermocouples controlling the heaters in relation to the indenter and the sample. This depends essential on the design of the instrument but also upon the thermal properties of the specimen and the indenter assembly. The actual temperature of the specimen beneath the indenter tip was therefore compared to the nominal temperature by conducting indentations into a thermocouple attached to the specimen surface. This enabled the actual temperature of the indenter tip to be measured directly from the thermocouple on the specimen surface. As can be seen (Figure 12) the actual temperature of the specimen surface can be significantly lower than the nominal temperature set on the instrument. The difference between the nominal temperature and the actual measured temperature was found to be less significant in highly conducting specimens such as copper and steel and most significant in ceramics (JGC118 and JGG007) and polymeric materials which act as thermal insulators.

The temperature of the sample surface can be measured during an actual experiment by attaching a thermocouple to the edge of the sample allowing the material to be indented at the centre of the specimen. This can be highly accurate for thin, highly conductive materials such as copper, steel or aluminium with uncertainties in temperature of less than 1%. However, care must be taken using this technique with thermal insulators such as polymers and ceramics as temperature can vary significantly across the surface of the specimen.

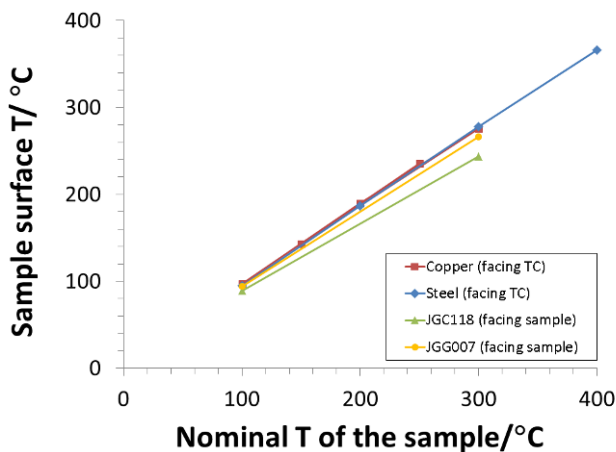


Figure 12: Sample surface temperature as a function of the nominal temperature set in the temperature controller of the sample.

An alternating procedure has therefore been developed in which the temperature difference between the sample surface and the indenter tip is calibrated by monitoring the change in temperature that is observed when an indenter is pressed into a thermocouple that is attached to the specimen hot-stage. By monitoring the change in temperature that occurs when the indenter approaches an actual specimen it is possible to determine the temperature of the specimen from the temperature of the indenter tip and the change in temperature that occurs as it enters the specimen. The overall uncertainty of the instrument was found to be approximately 5% over a range of temperatures from room temperature up to 300°C. Guide-lines and a scientific paper describing the procedures that should be used to calibrate high temperature nanoindentation instruments have been produced by NPL.

By using the high precision indentation measurement setup at NPL, creep data obtained from aluminum alloy (6082T6) specimens using high temperature nanoindentation was then used to validate the nanoindentation technique by comparing the data to creep results obtained from conventional uniaxial creep measurements. Creep compliance values obtained from the aluminum specimen using the nanoindenter at 23, 100, 200 and 315°C demonstrated, as would be expected, an increase in the creep rate as the temperature increased. However, to examine whether this could be used to conduct accelerated testing it was necessary to establish the time-temperature equivalence to relate short-term high temperature creep tests to the long-term low temperature creep. This was conducted using the Arrhenius relationship to relate the activation energy ϕ , and the absolute temperature T to the time t :

$$\ln(t) = \left(\frac{-\phi}{R} \right) \left(\frac{1}{T} \right) + \ln A$$

where A is a constant and R is the universal gas constant (8.314 J mol⁻¹).

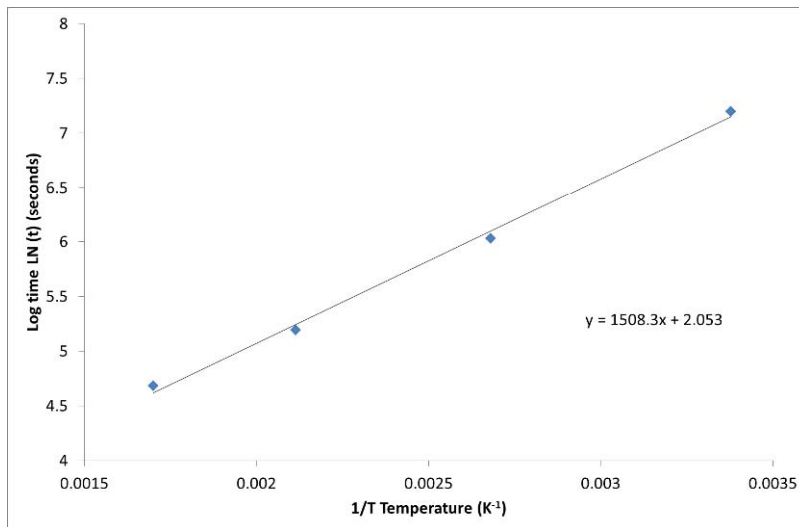


Figure 13: Arrhenius plot of $\ln t$ versus $1/T$ for indentation creep data, where t is the time at which the compliance reaches its critical value $4 \times 10^{-9} \text{ Pa}^{-1}$. The linear relationship indicates that the indentation creep behaviour obeys the Arrhenius relationship.

Plotting $\ln t$ against $1/T$ (Figure 21), it can be seen that a good linear fit is obtained for the indentation creep data for aluminum, indicating that the Arrhenius relationship can be used for accelerated indentation creep tests. The Arrhenius equation also allows the activation energy ϕ of the creep to be determined by dividing the slope of the Arrhenius plot $\ln t$ against $1/T$ by the universal gas constant R ($8.314 \text{ J}^{-1} \text{ mol K}$). The activation energy obtained from the indentation data was calculated to be 13 kJ mol^{-1} which is consistent with the values obtained in pure aluminum at lower temperatures ($<400 \text{ K}$) by Ueda et al [6], approximately 20 kJ mol^{-1} .

the nanoindenter at elevated temperatures; to achieve accurate temperature control of non-thermally conductive materials such as polymers; to obtain reliable creep data from elevated temperatures using nanoindentation; and to conduct accelerated creep testing using elevated temperatures.

The work conducted in this project has developed the procedures that are required: to accurately calibrate

3.2.3. Conclusion

NPL, the UK's National Measurement Institute (NMI), developed a new method to calibrate nano-indentation equipment at elevated temperatures, including measurements of displacement, frame compliance and area function. An uncertainty budget was established using the procedures for determining uncertainty detailed in the BIPM [Guide to the Expression of Uncertainty in Measurement](#) (GUM), incorporating both uncertainties introduced by the measurement device and the environment in which the device is used. The research revealed the two most important sources of uncertainty were caused by uncertainty over the size of the area of contact between the instrument indenter and the sample, and differences in sample stiffness. To address these, a method was devised to accurately estimate the area of contact from measurements of indenter depth, using an area function determined by scanning the indenter tip using atomic force microscopy.

The objective was achieved, as the calibration approach and uncertainty budget allowed measurements to be made from room temperatures up to 300°C , with an overall uncertainty of approximately 5%. Guidelines and a scientific paper describing the procedures for calibrating high-temperature nano-indentation instruments have been published by NPL.

3.3. Objective 3: Measurement of time and temperature dependent behaviour of samples by optical interferometry with an uncertainty below 0.5 nm for measurement length up to 300 mm. The time scale of the measurements can be over a year and the temperature range allows measurements from 15 °C to 30 °C.

3.3.1. Introduction

The main objective of the project was the investigation of long-term dimensional and thermal stability of materials and joints by interferometry and indentation techniques. The primary step to guarantee dimensional stability is a stable environment. When parameters like temperature, pressure and humidity are

stable or, at least, are known very well, repeated length measurements provide information about the intrinsic stability of a material.

With growing precision in the assembly of ultrahigh-precision instruments, there is a need to investigate not only the stability of materials but also of connections (joints). Generally, a joint consists of different materials, interacting at an interface or interlayer. The behaviour of a joint is not only the sum of the parts behaviour but also of their interaction. Screws or glue can cause unpredictable relative movements. In contrast to measurements made on materials, e.g. glass ceramics, there is little published knowledge concerning the long-term stability of joining techniques with a precision of a few nm or even below.

In addition to the newly developed interferometer at VSL and the optimized indentation equipment at NPL, existing equipment at PTB was used for the measurements. At PTB, interferometric length measurements with sub-nm precision are available using instrumentation similar to gauge block interferometers. Measurements were performed at PTB's interference comparator INKO6 (air), Precision Interferometer PI (vacuum) and the Ultra Precision Interferometer UPI (vacuum). Digital imaging phase stepping interferometry is applied, with three stabilized lasers of different wavelength being used subsequently in the measurements.

The interferometric measurement of sample stability with highest accuracy is a differential measurement of two parallel surfaces, one on the sample and the second on a reference, it is necessary to keep the parallelism of the surface during the joining process. One main task of the project was therefore to develop techniques for the sample preparation, as described in the following paragraph. Additionally samples were prepared, which were measurable also on the NPL indentation instrument.

3.3.2. Sample preparation for interferometric measurements

At the PTB Gauge Block (GB) Interferometers new methods for the determination of the relative motion of connected gauge blocks have been implemented. Each phase topography was analyzed in a number of steps. In the case of only one longitudinally connected GB to be investigated, the face centre and orientation of the GB are determined. A coordinate frame which rotates with the GB alignment is generated: h notates the distance in the (horizontal) direction along the GB, and v (vertical) across the GB. Regions of interest (ROIs) are generated on the top GB surface and in defined distances along the v direction on the platen. When obstructing objects like screws are present, an additional shift in the h direction is necessary.

In the case of *longitudinal joints*, the desired "joint length" is simply the height difference between the GB top face (ROI centre), z_1 , and the interpolated platen below the GB, $z_{P,1}$, at the same lateral position: $l = (z_1 - z_{P,1})$.

This also holds for specimens with cylindrical symmetry, where the top ROI is a circle and the platen ROI a concentric ring, and the height difference is taken in the mathematical centre.

For *lateral joints* the height difference between the top GB faces 1 & 2, characterizes the lateral stability:

$$l_{rel} = (z_2 - z_1) \square z' \cdot (v_2 - v_1); \quad z' = \partial z / \partial v.$$

Because the difference $(z_2 - z_1)$ has to be corrected for alignment rotation, a tilt, z' , has to be determined: the orientation of the platen in a continuous and flat area (cf. Fig. 4c). The angle difference between the GB ROIs was observed to check for the assumption that all parts adhere to a rigid-body rotation or if mutual tilting occurs. The dominating error source for l_{rel} is the uncertainty of z' . As observed from the laterally screwed joint drift curve, l_{rel} is subject to a scatter of less than 4 nm.

Specialized, inorganic joining techniques have been developed in order to assemble optical components for ultrahigh-precision instruments. The demonstrators supplied by Fraunhofer IOF (FhG) are standardized, representative case studies with an alignment capability ranging from 3 to 6 DOF and were characterized on the basis of absolute length measurements performed at PTB. Also, representative screwed (bolted) and glued connections of gauge blocks (GBs) were manufactured, according to specifications required for high-precision measurements of length and orientation in all relevant directions (parallelism within 4 arcsec).

The validation of Picodrift Interferometer measurements (VSL) by absolute length measurements (PI, PTB) was realized by the use of reference artefacts with differing drift properties: 1. zero drift (silicon single crystal), 2. low drift (glass ceramics with slow cooling) and 3. high drift (glass ceramics with fast cooling). The choice of glass ceramics with $|CTE| < 10^{-7} / K$ was to have known drift rates, while the length is unaffected by

the temperature drift. After the samples had been measured at PTB at 20°C, they were removed from the platen and a 2nd Al coating was added. The samples were packed in a multi-shell thermo-isolation box and transferred personally in order to guarantee that the temperature does not significantly exceed 20°C. After being measured with the Picodrift Interferometer, they were wrung to the reference platen again at PTB. The re-wringing introduces an absolute length shift of a few nm, therefore, drift curves remain un-joined.

Length and angles were measured normally and laterally to the connection interface several times within a period of 1-2 years. To prevent phantom drift by inherent material instability from influencing the analysis of joints, the stability of the steel GBs was also investigated. The GBs have rectangular end (measurement) faces (mostly of 9 mm x 35 mm) and are made of steel (Fig. 2a) or single crystal silicon. Two GBs were connected to each other, in the case of *longitudinal* joints at the (polished) *end faces*, and in the case of *lateral* joints at the (unpolished) *side faces*. In the second case, a problem results from the fact that GBs have very parallel end faces, but the end and side faces are only guaranteed to be perpendicular within ±50 µm (ISO 3650). Therefore, joints were aligned in an auxiliary interferometer in order to achieve parallelism. In each case one of the end faces was attached to a flat platen (made from the same material).

For the *advanced joining techniques*, silicatic bonding, AuSn laser-based thin-film soldering and Solderjet Bumping, longitudinal sample joints consist of a small parallel optical mirror plate ($l = 5$ mm) of 10 mm Ø which is joined to a base mirror of 25 mm Ø (Fig. 6a). One translational DOF and tip/tilt were investigated in the PI. Specimens were measured repeatedly at 20 °C. Also a thermal cycle was carried out with: 20 °C, 10 °C, 40 °C, 30 °C and 20 °C. The absolute length here represents the optical step height of the small mirror's front face in relation to the surface of the large mirror including the thickness of the joint. Areas of the surfaces in which the phase topography was to be analyzed have a protected Al coating. The samples were made of fused silica which reduces the effect of the temperature on the length due to a CTE of $\approx 5 \times 10^{-7} \text{ K}^{-1}$.

Thermocouples were attached to each specimen (Fig. 2a). The length was extrapolated to exactly 20 °C, involving a CTE for steel of $(11.5 \pm 0.5) \times 10^{-6} \text{ K}^{-1}$ and $2.56 \times 10^{-6} \text{ K}^{-1}$ for Si. The estimated standard uncertainties of length changes near 20 °C are 3 nm (INKO6) and 1 nm (PI, UPI) or less (e.g. for fused silica). The orientation was determined from a linear fitting of continuous regions which are more or less flat. The area should be as large as possible in order to minimize the uncertainty originating from the surface roughness. The uncertainty for the angle measurement on lapped steel surfaces was estimated to $u(z') < \pm 0.2 \text{ arcsec} = \pm 1 \text{ } \mu\text{rad}$, and on fused silica to $< \pm 0.1 \text{ arcsec}$.

3.3.3. Measurement results

The long-term dimensional and thermal stability and dilatation of materials and joints, produced with techniques as wringing, screwing (bolting), gluing, bonding and soldering, has been investigated. Techniques were developed and specimens were manufactured from GBs, exploiting the parallelism and flatness of the surfaces and allowing for the joints to be investigated in different length measuring interferometers as used for GB calibration. Accuracies below 1 nm longitudinal and 2...4 nm laterally were achieved. Steel GBs showed thermally-induced instability when heated above 30 °C. After repeated absolute length measurements at 20 °C during over 1 year, thoroughly manufactured screwed joints are stable in at least 5 DOFs. They are also stable concerning thermally-induced drift by a temperature change of ±10 K. Adhesive joints can behave very differently, depending on curing and humidity absorption but also on the geometry of the glue joint. A wedge angle leads to instability of length and angle, which hints to the importance of producing a very symmetric and parallel glue distribution without squeezed-out blobs, in order to optimize the stability of adhesive joints. Highest stability is obtained for a gap distance below 1 µm and for hard contact with surrounding epoxy. The unfunded partner Fraunhofer IOF utilized our research to specify the stability of their advanced joining techniques. CTE measurements show how the geometry of the interlayer affects the thermal dilatation of joints.

Drift Analysis: In order to describe the length measurements at 20 °C as a function of time and model the drift of the low-drift glass ceramics GB, an empirical fit function (scaling relation) was chosen:

$$\Delta l(t) = l - l(t_0) = \Delta l_\infty \left[\left(\frac{t_0}{t} \right)^\beta - 1 \right]; \quad \dot{l}(t) = -\Delta l_\infty \frac{t_0^\beta}{t^{\beta+1}} .$$

Time t is counted from the end of heat treatment, and $\Delta l = 0$ holds for $t = t_0$. Fig. 14b) shows the measured length (dots) after heat treatment, and fit (thick), Fig. 14c) shows the derived drift rate. The fit parameters are: $\Delta l_\infty = 23.2$ nm (total drift), $\Delta l = 0.16$, $t_0 = 8.57$ d; total length includes offset length: $l(t_0) = 74,862,859,2$ nm.

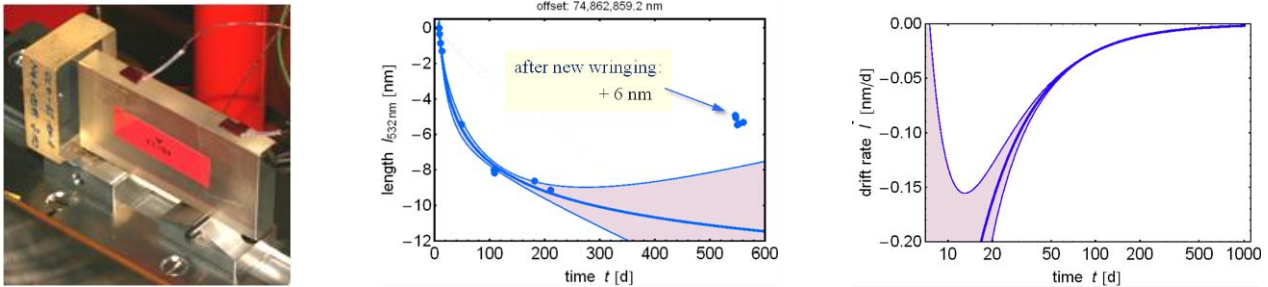


Figure 14: a) Low-drift artefact, b) length change Δl , c) drift rate $i(t)$ (time derivative), with confidence intervals

Wringing and thermal stability of steel gauge blocks: The probably most stable joining technique is wringing in which very flat surfaces are directly connected via molecular adhesion forces. Two stacks of each 2 x 12.5 mm steel GBs were wrung onto a steel platen (Fig. 15a). After the length of the two stacks was measured within ≈ 1 year at 20 °C, the temperature was varied between 10 °C ... 40 °C for CTE determination. Both stacks, measured again at 20 °C, showed a length increase of 6 nm to 7 nm which relaxed to the original length during the following weeks (Fig. 15b) with an average relative drift rate (related to the total length) of

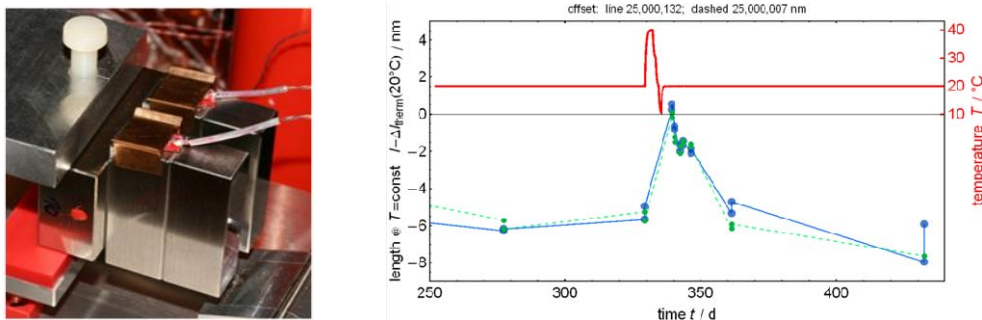


Figure 15 a) Stacks of wrung steel GBs; b) length changes at 20°C (below), temperature history (upper red line)

about 10^{-8} per day. This was an unexpected result which shows that the stability of the joined parts has to be considered in order to measure “the stability of a joining technique” from measurements of the whole joint – otherwise, phantom instability may result.

Screwed (bolted) connections: The *longitudinal* joint (Fig. 16) consists of a 12.5 mm steel GB bolted with two M3 screws and a torque of 1 Nm to a platen. A *lateral* connection of two steel GBs was produced (Fig. 17). The mutual tilt was minimized by a 10 μ m precision gauge sheet on one side between the GBs and one screw given a torque of 0.5 Nm. No drift or tilt was detected during 600 d. Temperature was cycled between 10...30 °C, which did not cause any change, back at 20 °C. Preparation had to be done carefully: GBs, screws, nuts and washers are perfectly clean and fit smoothly into each other. Any dust or friction could lead to stress relaxation and instability.

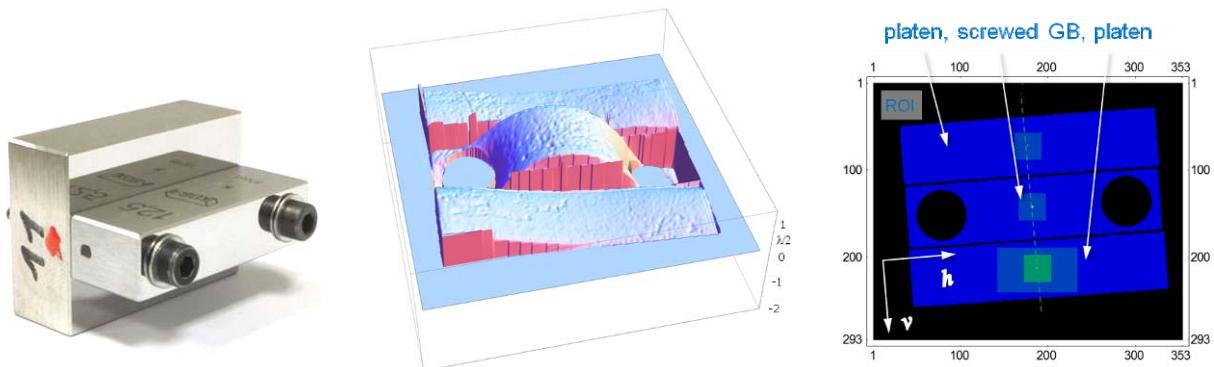


Figure 16 a) Longitudinal screwed joint; b) phase topography, $\square = 532 \text{ nm}$; c) ROIs for phase analysis

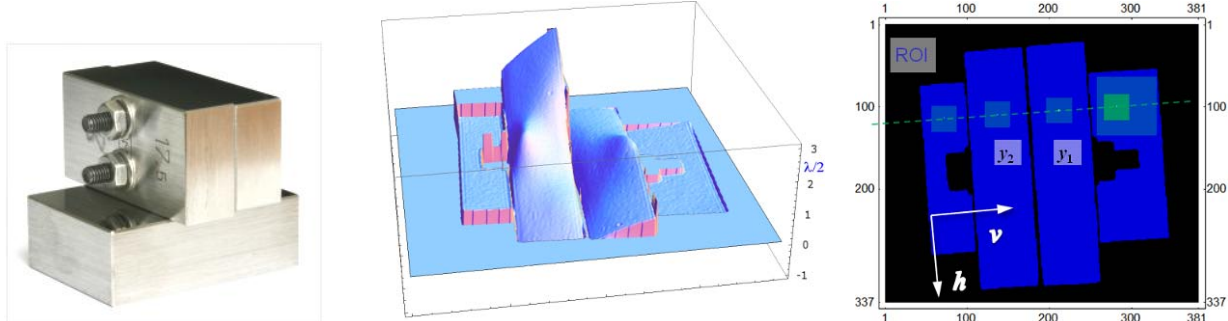


Figure 17 a) Lateral screwed joint; b) phase topography, $\square = 532 \text{ nm}$; c) ROIs for phase analysis, interpolation

Adhesive connections: Two steel GBs of 5 mm and 15 mm nominal length were *longitudinally* joined by a synthetic resin (*Crystalbond 509*) layer of $d = 152 \text{ nm}$ thickness (which is small enough to avoid dimensional change) using a dilute solution. Both GBs were heated to $150 \text{ }^\circ\text{C}$ for the resin to melt. The heat treatment caused an instability of the GBs with an initial drift rate of $\approx -10^{-8} / \text{d}$. This was confirmed by measurements performed after the joint was broken and the GBs were measured without the resin. At $t = 190 \text{ d}$ the total drift rate had reduced to a half of the initial rate. When compared to the results in 4.1, where the highest temperature was $40 \text{ }^\circ\text{C}$, we find that an increase of the annealing temperature increases the total amount and duration of the relaxation.

When two 15 mm GBs made of Si (thermally stable) were joined in the same way, length and angles stayed constant for 1 year. A temperature raise to $30 \text{ }^\circ\text{C}$ for 1 d resulted in a permanent length increase of $+4 \text{ nm}$.

Two 12.5 mm steel GBs were longitudinally joined by a $(8.2 \pm 0.4) \mu\text{m}$ layer of 2-component epoxy *UHU+Endfest300* at $20 \text{ }^\circ\text{C}$. A length relaxation by 25 nm (epoxy curing) was detected during 100 days (Fig. 18a). Afterwards the specimen was heat-treated at $50 \text{ }^\circ\text{C}$ for 3 days, which resulted in a length increase of 10 nm at $20 \text{ }^\circ\text{C}$, followed by a relaxation by -16 nm during another 170 days. The following length increase is probably the result of moisture swelling of the epoxy, because the specimen was measured and stored in air with humidity of 40 %... 60 % so that moisture constantly diffuses into the glue joint. No tilting was detected.

Two steel GBs were *laterally* joined by epoxy. Significant changes of length and orientation were measured (Fig. 18b). With the help of an FEM model it was concluded that the adhesive layer is not parallel but varies in thickness by $\approx 33 \mu\text{m}$ along the z direction, which not only leads to a change of the respective tilt angle when the adhesive volume changes, it also leads to a lateral movement as a result of the tilting. Another source of instability is caused by the vacuum: a non-uniform adsorption layer on the glued GB surface had formed originating from squeezed-out epoxy. A removal of the layer resulted in an increase of \square_{GB2} by 1 arcsec.

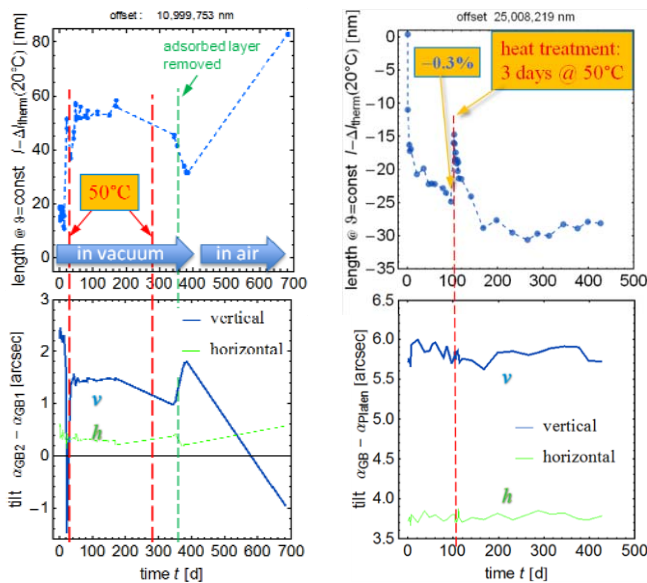


Figure 18: Adhesive joints: length at 20°C (above), tilt angle at all temperatures (below); heat treatment marked by red dashed line; a) longitudinal; b) lateral, removal of adsorbed layer marked by green dashed line

in vacuum). After storing the joint in air, the length increased by $\approx +0.5$ nm/d (moisture swelling).

Silicatic Bonding: Parallel plates made by the Fraunhofer IOF of fused silica were joined by a thin SiO₂ bonding layer of $d \approx 100$ nm (which does not influence the overall thermal expansion). The two investigated joints showed a length reduction of -3 nm. A possible reason results from the bonding process: water is driven out by a heat treatment. But, some water may evaporate later, leading to a volume decrease. After 100 days no change was measured anymore. No change of orientation and no influence by the thermal cycle on length or orientation were detected.

The thermal expansion of the specimens can be described by Taylor approximations of 2nd order, the respective equations are given in Table 1. The resulting CTE value at 20 °C is $(4.66 \times 10^{-7} \pm 9.8 \times 10^{-9})$ K⁻¹.

AuSn laser-based Thin-film Soldering: The 80Au20Sn alloy has a CTE of 16×10^{-6} K⁻¹ at 20 °C, with an average solder film thickness (8.9 ± 0.5) μm. Therefore, the film is expected to give a contribution to the total CTE of $\approx 3 \times 10^{-8}$ K⁻¹. The total CTE of the thin film-soldered joint (linear term in Table 1) is $(5.55 \times 10^{-7} \pm 9.6 \times 10^{-9})$ K⁻¹ and therefore $(9 \pm 2) \times 10^{-8}$ K⁻¹ higher than that of the silicatic bonding specimen, which is slightly more than the AuSn film contribution.

The three specimens manufactured by the Fraunhofer IOF were investigated and showed length increases between +1 and +5 nm during 400 days. No change of orientation and no influence by the thermal cycle were detected.

SnAgCu Solderjet Bumping: Three patches of solder bumps from the Fraunhofer IOF were placed between the silica cylinders and are bridging a gap of ≈ 100 μm. The Sn₃Ag_{0.5}Cu solder alloy has a CTE of 22×10^{-6} K⁻¹, but the bumps give a larger contribution to the total CTE, which was measured to $(1.47 \pm 0.01) \times 10^{-6}$ K⁻¹, than calculated from the gap distance (0.43×10^{-6} K⁻¹), because the bumps are thicker at the rim of the top plate.

The Solderjet-Bumped specimens show larger instability, certainly due to the larger solder gaps. The specimen E-PTB_05 which was thermally-cycled between 10...40 °C at the beginning showed a length increase by $\approx +25$ nm (Fig. 19b). A tilting by 0.4 arcsec was measured, directly related to the thermal cycling, and another 0.5 arcsec during the following 270 days. Another specimen showed a length increase by +10 nm and a tilting by 0.5 arcsec during 270 days without heat treatment. A following temperature increase to

Spacers were used to produce a hard contact between the GB end faces. 10 Vol.% of *spherical glass beads* (nominal size distribution \varnothing 0...50 μm) were added to the epoxy. The adhesive layer had a final thickness of (70.6 ± 0.3) μm, which approximately coincides with the largest glass beads observed under the microscope. A curing relaxation by nearly -100 nm was observed during ≈ 50 days, but followed by a length increase (moisture swelling) by $\approx +80$ nm during 400 days. The effects are much larger than of the pure epoxy joint, probably because of the much larger glue gap. Also a glue gap of only 13 μm was produced using smaller glass beads and compressive force but with similar results. Moreover, the measurements show a tilting of up to 2 arcsec, possibly by moisture swelling of the un-symmetric joint with squeezed out epoxy. The CTE of the joint is $(13.13 \pm 0.02) \times 10^{-6}$ K⁻¹ and $\approx 1.5 \times 10^{-6}$ K⁻¹ larger than of GB steel, influenced by squeezed-out glue.

A *hard contact* between the end faces of silicon GBs was approached without adhesive in between. The low-outgassing epoxy *Torr Seal TS10* acts on the periphery of the contact interface. The total curing relaxation is ≈ -10 nm (in

40 °C for 2 days resulted in a length reduction by –6 nm and an increase of the drift from (0.02 ±0.01) nm/d to 0.08 nm/d (Fig. 6c). Both specimens showed a slowing down of the drift rate (relaxation).

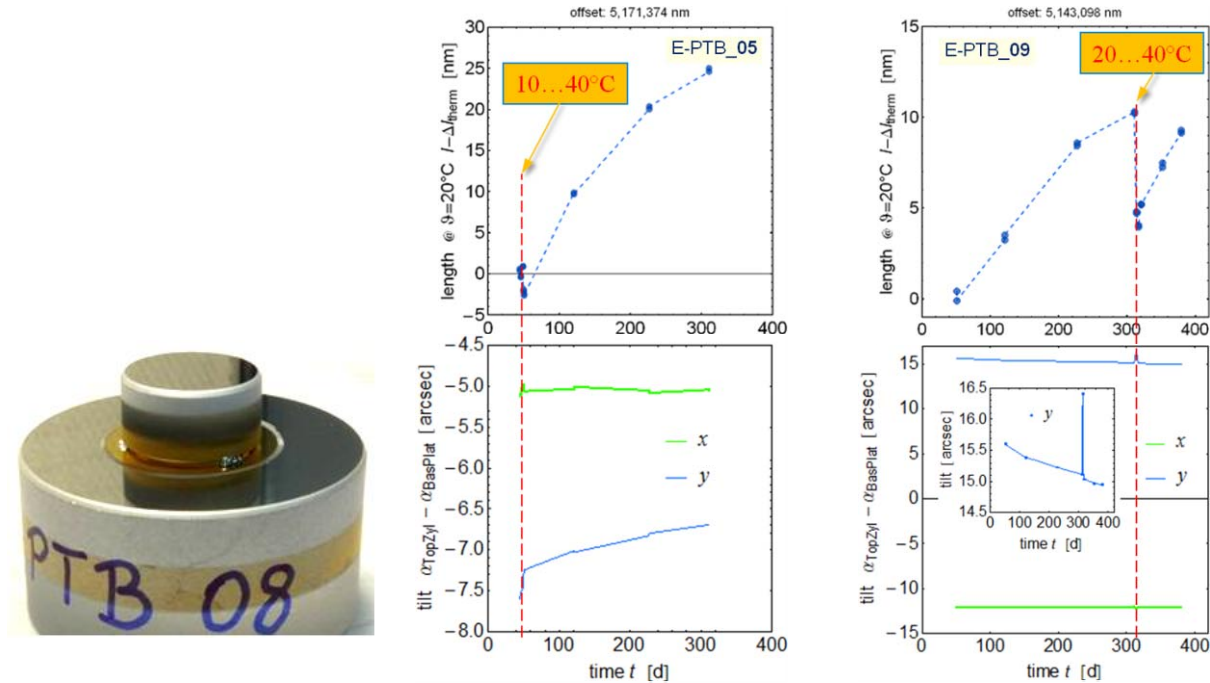


Figure 19 a) Solderjet Bumping specimen; length change (above) and tilt angle (below);
 b) thermal cycle at beginning; c) thermal treatment after 300 days (marked by red dashed line)

Table 1. Taylor approximation of 2nd order for the thermal expansion: $\Delta l_{therm}/l =$

Specimen	Linear term	Quadratic term	Temperature
2x12.5mm steel GB1	$(11.478 \times 10^{-6} \pm 1.9 \times 10^{-9}) K^{-1} \cdot (\Delta T / 20^\circ C)$	$+ (1.20 \times 10^{-8} \pm 1.2 \times 10^{-10}) K^{-2} \cdot (\Delta T / 20^\circ C)^2$	10°C...40°C
2x12.5mm steel GB2	$(11.152 \times 10^{-6} \pm 1.9 \times 10^{-9}) K^{-1} \cdot (\Delta T / 20^\circ C)$	$+ (1.09 \times 10^{-8} \pm 1.2 \times 10^{-10}) K^{-2} \cdot (\Delta T / 20^\circ C)^2$	10°C...40°C
Silicatic Bonding	$(4.66 \times 10^{-7} \pm 9.8 \times 10^{-9}) K^{-1} \cdot (\Delta T / 20^\circ C)$	$+ (1.2 \times 10^{-9} \pm 6.8 \times 10^{-10}) K^{-2} \cdot (\Delta T / 20^\circ C)^2$	10°C...40°C
Thin-film Soldering	$(5.55 \times 10^{-7} \pm 9.6 \times 10^{-9}) K^{-1} \cdot (\Delta T / 20^\circ C)$	$+ (1.7 \times 10^{-9} \pm 6.1 \times 10^{-10}) K^{-2} \cdot (\Delta T / 20^\circ C)^2$	10°C...40°C
Solderjet Bumping	$(1.472 \times 10^{-6} \pm 9.7 \times 10^{-9}) K^{-1} \cdot (\Delta T / 20^\circ C)$	$+ (2.6 \times 10^{-9} \pm 7.3 \times 10^{-10}) K^{-2} \cdot (\Delta T / 20^\circ C)^2$	10°C...40°C

The performance of the VSL Picodrift interferometer for configurations with samples and the refractometer cell present has been established as well. A selection of relevant reference standards and representative samples, provided by the project partners PTB and FhG, is presented in Figure , including a low thermal expansion gauge block (GB), two wrung silicon gauge blocks acting as the main reference standard, and two fused silica cylinders bonded together using varying techniques. The performance ranges from 6 pm, 15 pm, and 39 pm for an 1 second averaging interval, to 39 pm, 73 pm, and 88 pm for an 1 hour averaging interval, as measured for the ClearCeram GB, the wrung silicon GBs, and the bonded fused silica cylinders, respectively. The relative sample length as compared to the 75 mm length of the refractometer cell is 1, 0.67, and 0.23, for the three samples, respectively. The statistical results for these samples show that for optimal performance it is essential to match the length of the sample with the length of the refractometer cell. This is true for short averaging intervals, since the baseline noise is higher of the reference signal which is only required in case of sample length scaling. But even more so for longer averaging intervals, since drift intrinsic to the interferometer cannot be properly compensated for due to mixing of the drift signal with the refractive index fluctuation as measured over the entire refractometer cell length, as measured by the refractometer interferometer branch.

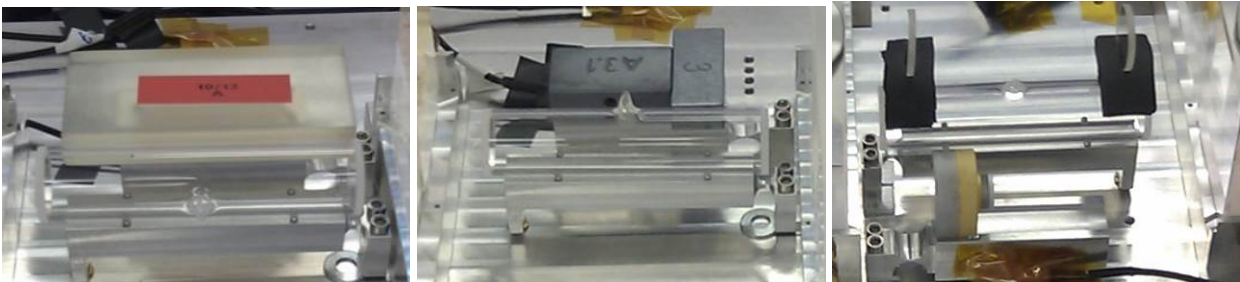
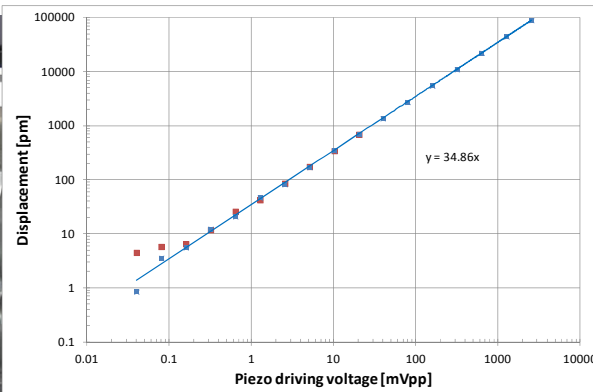
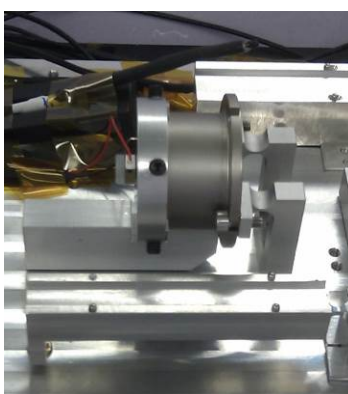


Figure 20. ClearCeram gauge block (left), wrung silicon gauge blocks (center), and bonded fused silica cylinders (right), as examples of measurements of materials and material connections.

Finally, the instrument has also been used to calibrate two piezo actuators to be used as a reference standard. As the actuation frequency can be isolated from the majority of interferometer noise, it is relatively easy to achieve a measurement uncertainty below 5 pm (figure 21). After calibration of a piezo actuator, the piezo has been used as a virtual reference standard in order to calibrate an atomic force microscope^[1], which was performed as part of the 7th framework programme project Aim4NP.



Vpp [mVpp]	300 S/s [pm]	30 S/s [pm]	norm. [-]
2,560	89,480		1.000
1,280	44,326		0.991
640	22,127		0.989
320	10,950		0.979
160	5,436		0.972
80	2,714		0.971
40	1,358		0.971
20.48	688.0	687.3	0.961
10.24	340.0	341.6	0.950
5.12	170.0	174.7	0.950
2.56	82.2	85.3	0.918
1.28	46.2	42.2	1.032
0.64	20.8	25.8	0.929
0.32	12.2	11.8	1.095
0.16	5.6	6.5	0.995
0.08	3.6	5.8	1.273
0.04	0.8	4.5	0.598
0	1.6	2.2	

Figure 21. Piezo actuator attached to a retroreflector on one side and fitted with mirror on the other (left). Actuator displacement as a function of peak-to-peak driving voltage (center). Measurement data (right) at two different sampling rates, with the sensitivity of the piezo normalised on the value corresponding to the maximum excursion in the last column.

Creep rates for a range of 5 different materials have been determined using nanoindentation at NPL for a database that has been developed by the consortium for designers of high precision engineering equipment (table 1). Values for the creep rate of specimens A-NPL-1C, C-NPL-7 and E-NPL-1 have been shown to be consistent with results obtained by PTB and VSL.

Table 1 Creep rates for materials determined using nanoindentation

Sample	Creep+drift rate measured	Comments
Sapphire	0.137 fm/second	Berkovich diamond indenter
Fused silica	0.365 fm/second	Berkovich diamond indenter
A-NPL-1C	-15.9 ± 20.2 fm/second	Spherical diamond indenter (R=5µm)
C-NPL-7	27.8 ± 25.1 fm/second	Spherical diamond indenter (R=5µm)
E-NPL-1	24.9 ± 15.3 fm/second	Spherical diamond indenter (R=5µm)

3.3.4. Conclusion

30 samples were manufactured, including samples with soldered, glued, and screwed joints to test joint stability. The objective was achieved, as sub-nanometer measurements of stability and dimension changes were successfully performed. As the properties and behaviour of the standardised samples is now known, they can now be used as transfer standards for other laboratories to assess the accuracy of their precision engineering and measurement equipment.

Additionally, based on the experience gained during this objective, PTB, the German NMI, can now offer sample preparation as a service. The samples can be used as transfer standards to allow R&D labs and instrument/equipment manufacturers to calibrate their measurement devices, as the performance of each sample is known and has been documented. The samples can be produced to meet specific environmental requirements, with parameters such as pressure, humidity, and gas composition tailored to customer needs.

3.4. Objective 4: Development of self-calibrating resistance temperature sensors by fixed points near 20 °C using alloys. To enable improved temperature measurement and control electronics in regard of sensor compatibility, control parameter determination and ease of use including a verification of long time stability of thermocouples

3.4.1. Introduction

In all precision engineering applications temperature is a critical parameter due to thermal dilatation of the used materials for the measurement systems as well as for the machine structure. Temperature gradients and the resulting bending of the parts and machine structures are making the temperature influences more complex. For highest precision requirements a stable and homogeneous temperature environment and therefore a high precision temperature measurement is essential. It is hence necessary to be able to measure the whole temperature field in the sensitive area of precision engineering tools. This includes the measurement of temperature in air, at the surface of parts, and if possible inside of parts. For precision temperature measurements near room temperature, normally platinum resistance thermometers (PRT) and increasingly thermistors are utilized. Due to the sensitivity of the resistance to vibration, mechanical shock or other stress a calibration at regular time intervals is required. The increased number of temperature sensors which typically is necessary in ultra precision engineering tools therefore causes a higher maintenance effort

The aim of the work in this project regarding temperature metrology was the development of an accurate, traceable and reliable temperature measurement system with low maintenance costs for the temperature range around room temperature. This measurement system had to support the other partners in the project and have to allow for a universal use in precision engineering. The existing measurement electronics had to be optimized and enhanced with control algorithms.

Within this project a approach using a self validating temperature sensor based on a miniaturized fixed-point cell with a suitable phase transition temperature of about 20 °C was investigated. As no pure material with a melting point near 20 °C is available, appropriate alloys had to be investigated.

To measure the usually small temperature difference between the resistance thermometer and different measurement points in precision engineering tools, thermocouples are an interesting choice. Investigations of long-time stability, sample variations and external influences were performed in the project.

3.4.2. Self-calibrating resistance temperature sensors by fixed points near 20 °C using alloys

To investigate the influence of the size of the fixed point cell for the reference point of the temperature measurement system, the miniaturization of the cells was carried out in two steps. In the first step the volume was reduced by a factor of 4 (slim cells) compared to a standard gallium fixed-point cell. With a further miniaturization (mini cells) a reduction of the volume by a factor of 280 was achieved.

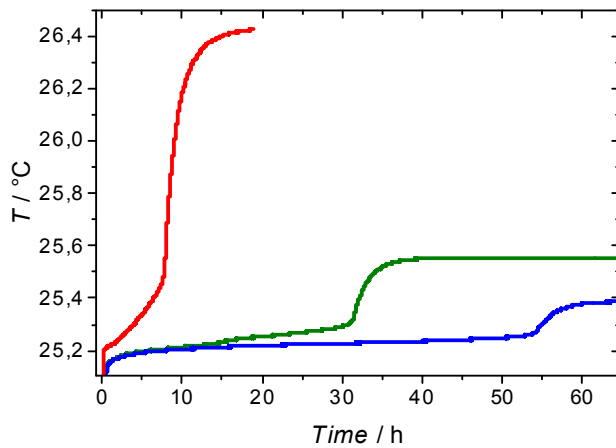


Figure 22: Melting curve variation of a slim Ga-Zn fixed-point cell after non-equilibrium freezing, for different temperatures of the thermostat (25,4 °C, 25,55 °C and 26,45 °C)

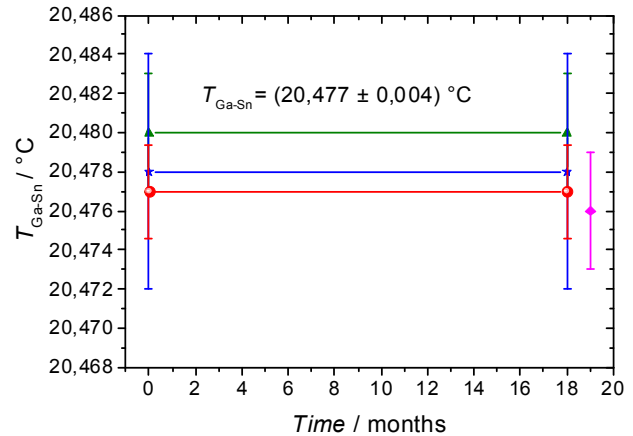


Figure 23: Reproducibility and long-term stability of the fixed-point temperature of 4 slim cells filled with a eutectic Ga-Sn alloy

Both types of cells were filled with gallium, and eutectic alloys of gallium with tin, zinc and aluminium (3-5 cells of each type). Compared with commercially available solutions the new setup (prototype) is about 10 times smaller and costs less than 10 %. By means of slim Ga-cells it was shown that the uncertainty contribution due to thermal/geometric effects can be reduced to about 0.2 mK. PTFE or PFA were identified as the most suitable crucible material.

The result for the Al-Ga system was very unsatisfactory and demonstrated that this alloy is not suitable as a fixed-point material. It was found that the Ga-Sn alloy is the most suitable one with a reproducibility (± 4 mK) which is about 5 times better than for the Ga-Zn (± 20 mK) alloy.

The investigations showed that there is an intrinsic physical limitation for further improvements. This is the influence of non-equilibrium thermal effects on the composition and structure of an eutectic alloy. Figure 22 exemplarily shows the large variation of the melting curve of a Ga-Zn binary eutectic produced under non-equilibrium conditions. It is shown that the variation of the fixed-point temperature is larger than 100 mK.

This confirms that uncertainties on the level of few millikelvin require a very large effort to produce homogeneous eutectic alloys at equilibrium thermal conditions. These findings were used to develop a prototype of a setup for an in-situ validation of temperature sensors by means of binary gallium alloys. It was demonstrated that with slim cells for the Ga-Sn system (20,477 °C) the target uncertainties of less than ± 5 mK can be achieved.

Further investigations have shown that the requirements for the temperature measurement systems are best fulfilled by two different solutions. The long-term monitoring of air or liquid temperatures should be carried out by the newest generation of hermetically sealed thermistors, whereas surface temperatures should be measured with mineral insulated thermocouples. Both sensor types require an individual calibration. For the validation of the long-term stability on a level of better than 1 mK the prototype setup together with slim Ga-fixed-point cells (29,7646 °C) can be used. An in-situ calibration at a temperature of 20,477 °C is possible with an uncertainty of about 4 mK.

3.4.3. Measurement of the stability of thermocouples near room temperature

An alternative to the use of PRTs and thermistors in precision engineering can be the use of thermocouples to measure temperature distributions in homogeneous environments as common in precision engineering. Thermocouples show a number of advantages.

- Small diameters of below 1 mm and a resulting small time constant. Therefore, thermocouples can be light and small, to prevent mechanical and thermal distortions at the measuring object due to the measurement itself.
- No self heating.
- At zero temperature difference, no voltage should be generated, so that it can be assumed that thermocouples are very stable over long time at small temperature differences.

The main limitation of thermocouples is the small sensitivity ranging from about 6 to 60 $\mu\text{V/K}$ depending on the material pairs used. To overcome this problem, a measurement system based on a relay switching box and a low noise amplifier has been optimized [8]. The measurement electronics could be optimized regarding error detection and the measurement noise was reduced by a factor of 3, due to the application of a newly developed preamplifier with less than 1 $\text{nV}/\sqrt{\text{Hz}}$ noise level. The amplifier was optimized for higher bandwidth, which allows in addition to a lower averaging time for the same noise level also for a reduced recovery time after switching between the channels. A new more user friendly interface has been developed and based on the modelling results at LNE and the TU Ilmenau a model predictive control algorithm has been selected to be used in the control computer. The software allows for generating output signals to characterize the system response of the system to be controlled to determine appropriate control parameters.

To validate the assumption regarding the long term stability and to check for the homogeneity of the characteristics of individual thermocouples as well as for the influence of external influences like temperature gradients or bending some test setups were realized.

For the stability test of the physical zero point thermovoltage, the two measurement points were brought in a good thermal contact, while electrical isolation was maintained. In the same way as described above the measurement points of the thermocouples were mounted on a small copper plate, which were then glued to common copper plates. One measurement point for all thermocouples was mounted on one copper plate. The other measurement points are mounted on the opposite side of a second copper plate with the same dimension. These two copper plates were screwed together for the stability measurements as shown in Figure 24. To obtain a more homogenous environment, the connected plates were located in an oil bath in a Dewar vessel. The Dewar vessel is isolated by Styrofoam layer, on which some winded water tubes are fixed. The whole setup is placed in a wooden box. A scheme of the setup is shown in Figure 25. A thick Styrofoam layer below a wooden top isolates the aperture of the Dewar vessel. Using a thermostat the temperature of the oil bath can be controlled accurately.



Figure 24: Two screwed copper blocks with thermocouples

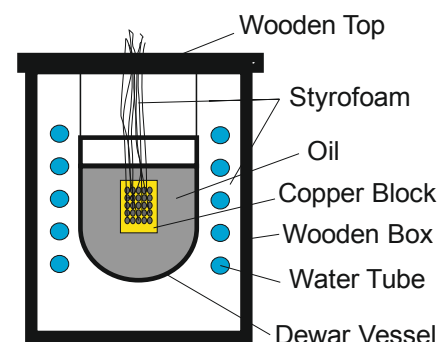


Figure 25: Oil bath

The whole setup was accommodated in a temperature-controlled laboratory room at a temperature of $(20.0 \pm 0.5) ^\circ\text{C}$. To check for the variations of the characteristic curves, a second oil bath, without water tubes, was used. After separation, the two copper blocks were put in each of the oil baths. By slowly heating up / cooling down of the first oil bath a difference in temperatures between all thermocouple pairs was generated and the variations of the characteristic curves of the individual thermocouples were observed. For tests of local heating of the thermocouple wires, a metal box was built with a heating resistor, where the wires could be heated over a length of about 50 cm.

To get an overview of the behaviour of different thermocouples a measurement system with 32 channels was installed. The thermocouples were made from different material pairs from different manufacturers and different wire dimensions. Two commercial thermocouples using thin films on an isolation foil. Unfortunately, in the oil bath the thin film of the latter thermocouples were dissolved from the foil after some time. A set of different manufacturing processes was used. One group of thermocouples were directly welded under inert gas from two feed lines of the same material and a connection line from the second material as shown in Figure 26a. Other commercial thermocouple pairs were welded together as given in Figure 26b, or connected over a clamp board with matched materials (Figure 37c) as well as by thermocouple connectors (Figure 26d). All feed lines were directly soldered to the relay circuit board.

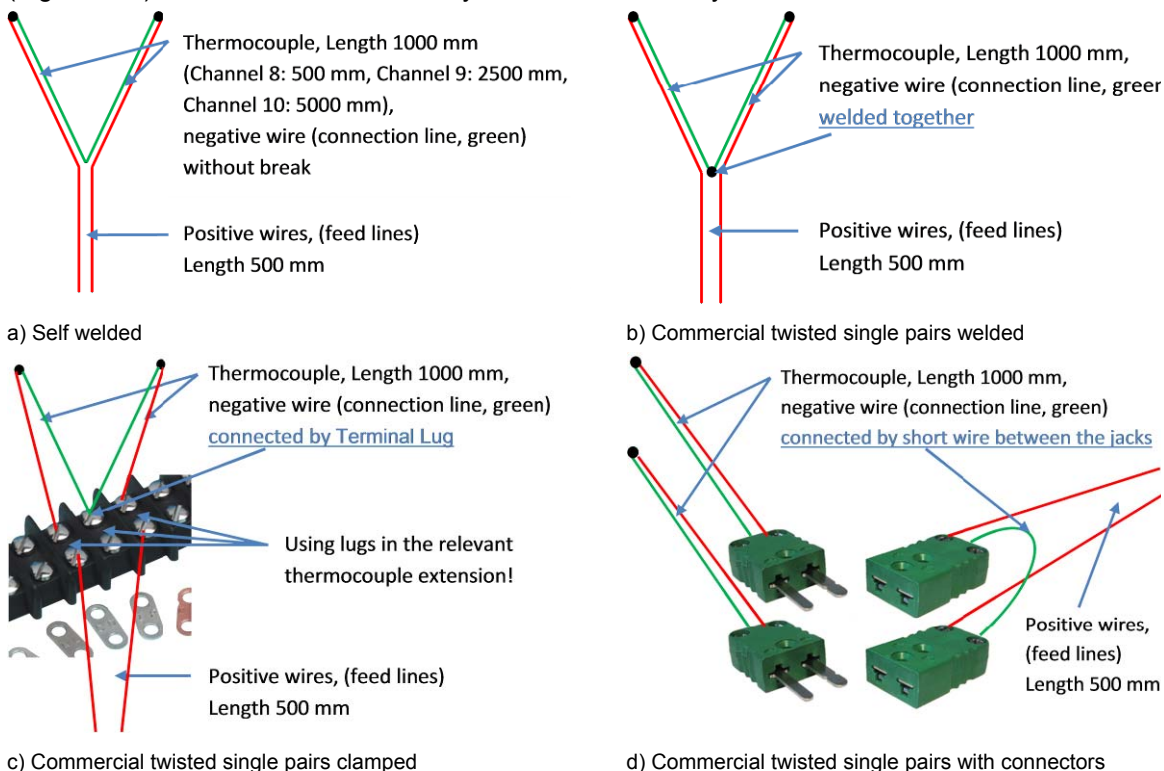
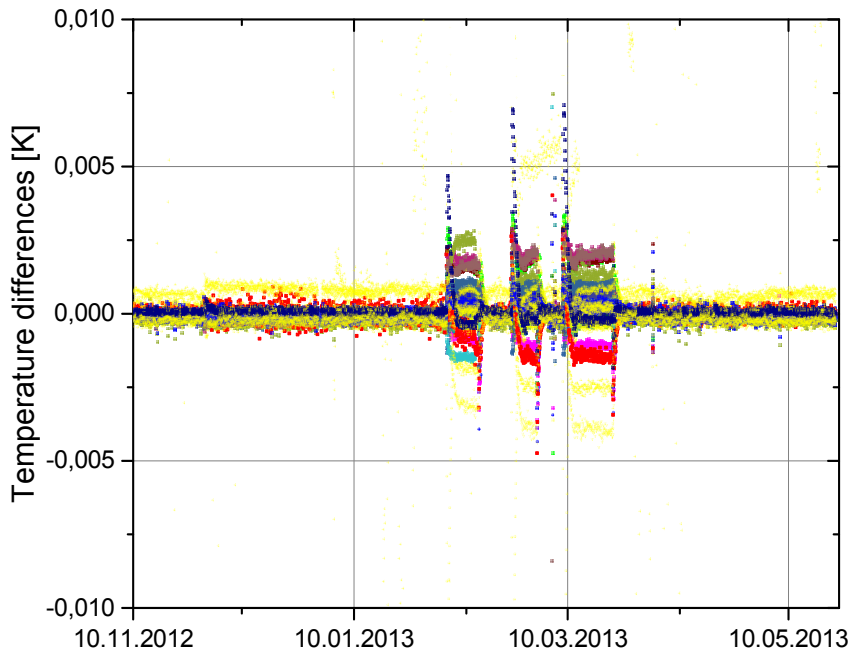


Figure 26: Manufacturing principles for the thermocouples

As thermocouples can only determine temperature differences, it is necessary to combine these sensors with a PRT to obtain an absolute temperature measurement. In this configuration the thermocouple only measures the difference of temperatures relative to a reference point with the PRT. To allow for in situ calibration of the PRT investigations of binary metal alloys were carried out with the aim of a miniaturized fixed point near room temperature.

Binary metal alloys are established as secondary fixed points for the calibration and self validation of contact thermometers between the fixed-points of the International Temperature Scale of 1990 at temperatures above 150 °C with typical uncertainties between 25 mK and 100 mK. Although several authors suggested the use of gallium alloys in the temperature range between 15 °C and 30 °C so far published investigations were inconsistent. Whereas in one investigation a very small uncertainty of 1.5 mK was stated for slim fixed-point cells based on Ga-Sn eutectic alloys, other authors could not confirm this finding. Therefore, within this project the suitability of 3 different binary eutectic gallium alloys (Ga-Al, Ga-Zn and Ga-Sn) for the self-validation of temperature sensors in the temperature range between 20 °C and 30 °C were investigated. The aims were the selection of the most suitable alloy and the determination and quantifications of the physical effects limiting the use of binary alloys. Further topics of the investigations were the minimization of parasitic heat losses by the thermal and geometric optimization of the fixed-point cells and the development of a transportable thermostat which allows fixed-point realizations under variable conditions (heating rates) and well defined cooling modes to produce eutectic alloys with optimum composition and structure.

An important point to use of thermocouples in precision engineering tools is the expected long term stability of the zero point, which then allows for a permanent mounting of the sensors in the tool. To allow for a better statistical evidence, 32 thermocouples have been selected as described above. The results of the long-term stability measurements of all 32 thermocouples over about 6 months are shown in Figure 27. The thermocouples with plug- or clamp connectors are shown light yellow. Each data point originates from a measurement cycle which was about 150 s for the 32 channels.



The stronger variations in February and March 2013 were caused by thermal gradients over the thermocouple wires generated by heating the oil bath about five Kelvin against the environment. This effect is discussed in more detail below. The variation of ± 1 mK observed from December 2012 to January 2013 for channel 19 (red curve) cannot be explained. It is noticed that this thermocouple is not specific with respect to any parameter.

Figure 28 shows values averaged over one day for some exemplary days with no external influences together with the standard deviations of these measurement results. A difference between different thermocouple types or geometries is not observed under the given environmental

Figure 27: Overall plot of temperature differences involving resulting from all thermocouples in a period of about 6 month

conditions and the measurement noise of the electronics. As already visible in figure 37, channel 19 from time to time shows an increased standard deviation,

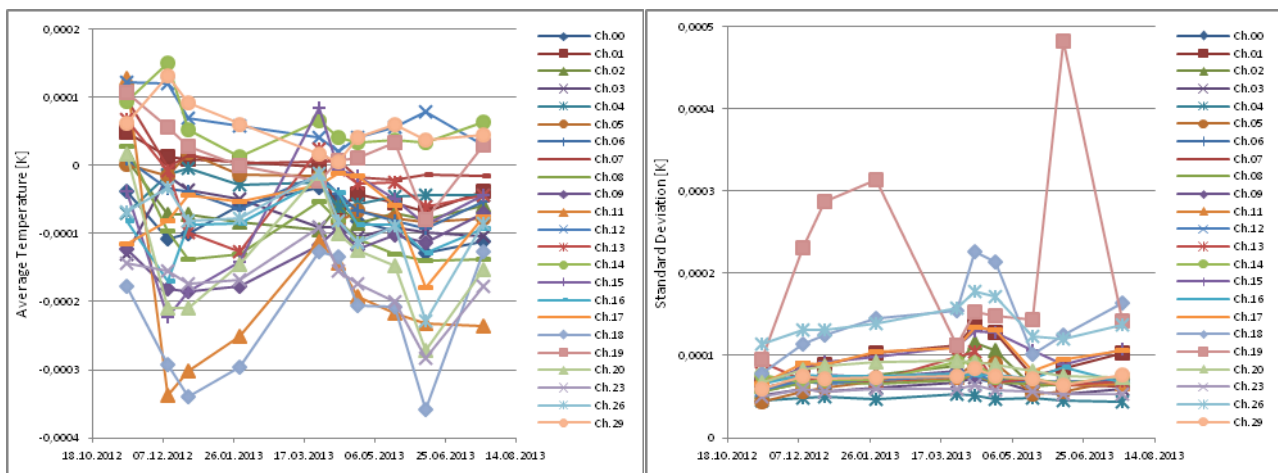


Figure 28: left) Values averaged over one day, right) the associated standard deviations on selected days over a period of nine months

To test the influence of mechanical stress on the thermocouples with at least 1 m wire lengths, the feed lines in the oil bath were bended with a radius of down to 2 mm. No effect on the physical zero point was observed. To check for the potential use of the thermocouples in a cable drag chain, the feed lines of the

longer thermocouples were subject to continuous motorized movement. Again, no effect onto the data signal was observed, not even on the average value. Only a slight increase of the noise level was observed, which we suppose to be caused by an increased electrical stray pickup caused by the motor, which was used to generate the movement.

More serious seems to be the effect of temperature gradients along the feed wires. To check for the influence of heat sources along the wires, a type T thermocouple situated in a closed box was heated along a path of about 50 cm. In Figure 29 the results are shown, if one arm with both wires (copper and constantan) was guided through the box. A temperature change of about 15 °C to 37 °C causes an error of nearly 7 mK. This value is sensitive to the position of the heater along the wire, and as shown in Figure 27 strongly varies dependent on the individual thermocouple. The results only guiding the copper wire through the heater box are shown in Figure 30. The copper wire was located in the heater box only within the two time slots A and B, indicated by the blue lines. In the time slot A a part of the wire near the switching box was heated, while in time slot B an area near to the constantan wire (see also Figure 26a) was in the heater. In the first case (A) nearly no effect is visible, which is different in the second case (B). We suppose that in the latter case the signal is affected by the heat flow to the constantan wire. However, the size of this effect is less by more than a factor of 10 compared to the situation when both wires are heated (Figure 29). Therefore, the copper wires seem to have much lower inhomogeneities compared to the constantan wires. It is noticed that constantan also has a higher resistance, which increases the measurement noise. Therefore, it is recommended, to keep the length of the constantan wire as short as possible.

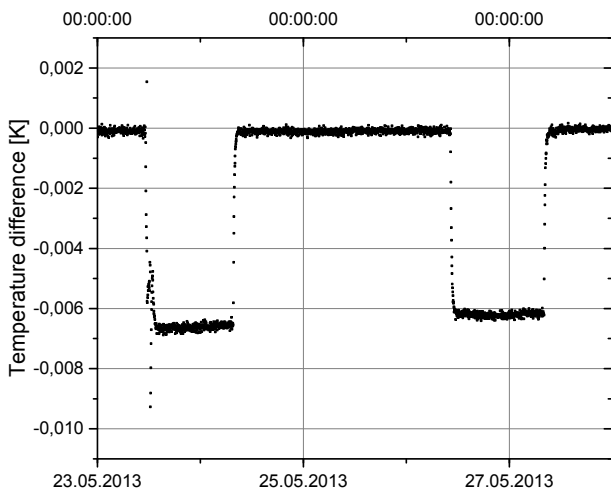


Figure 29: Type T thermocouple with both materials along 50 cm in a heater at 37 °C

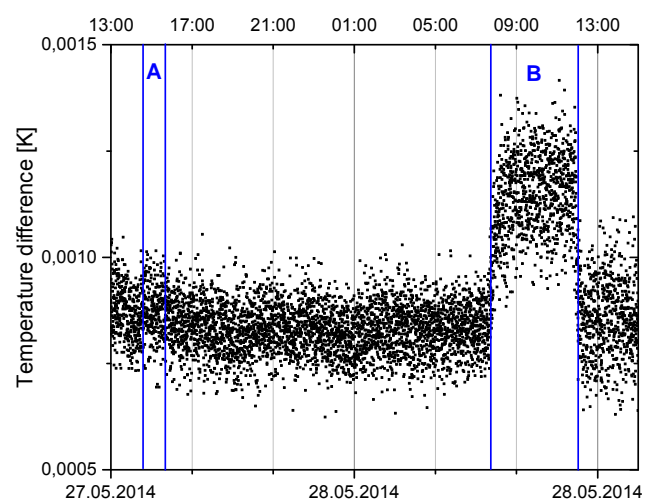


Figure 30: Type T with only the copper wire in the heater During time A a 50 cm part near the switching box

During time B the 50 cm near to the constantan wire.

To check for the influence of the characteristic curves of the individual thermocouples, the two copper blocks were separated and located in the two different oil bathes described above. One of the bathes was first heated up. During the subsequent passive cooling phase, measurements of all thermocouples were performed for a temperature range of about 0.2 K, which is reasonable large to describe the temperature stroke common in precision tools. The cooling rate varied from 0.35 mK/measurement cycle to 0.02 mK/measurement cycle. The total time for a measurement cycle involving 32 thermocouples was about 145 s. To visualize the variations of the different thermocouple types, the deviations from the common average is given in figure 19 for the type T, and in figure 20 for the type K thermocouples. Due to the sequential reading process, the measurements of the individual thermocouples are not exactly at the same time. As the copper block is cooling down during that time, there will be a real temperature difference in the readings. Compared to measurement times of a thermocouple in the middle of the reading cycle, the resulting correction is in the range of 0.1 mK for 0.15 K temperature differences of the oil bathes and more than a factor of 10 less near the zero temperature difference. Therefore, this effect can be neglected. The type T thermocouples were made from wires of the same manufacturer. Channel 10, which shows an offset of about 0.4 mK compared

to the other channels, is the one with the longest wires (5 m). Consequently, the offset could be induced by thermal distortions of the heater onto the environmental temperature. Over the relative small temperature range of 0.2 K deviations of ± 0.2 mK were observed.

For the type K thermocouples, wires from three different manufacturers were in use. The curves show a similar variation between the thermocouples from two of the manufacturers, but also clearly observable differences to the one thermocouple from the third manufacturer. Compared to the type T thermocouples the deviations were considerably larger even for the other group of thermocouples. For this reason, usage of type T thermocouples seems preferable.

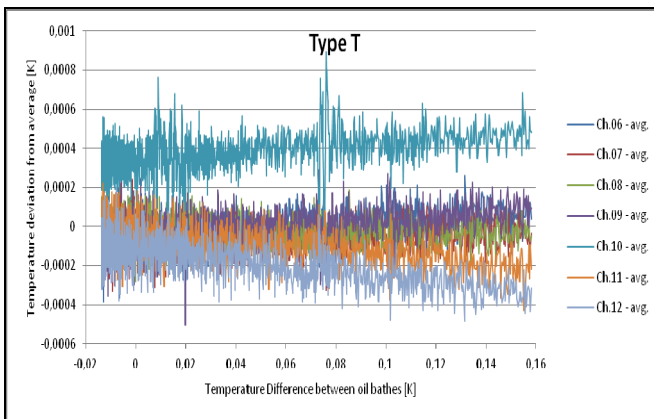


Figure 31: Characteristic curves of all welded type T thermocouples over about 0.2 K

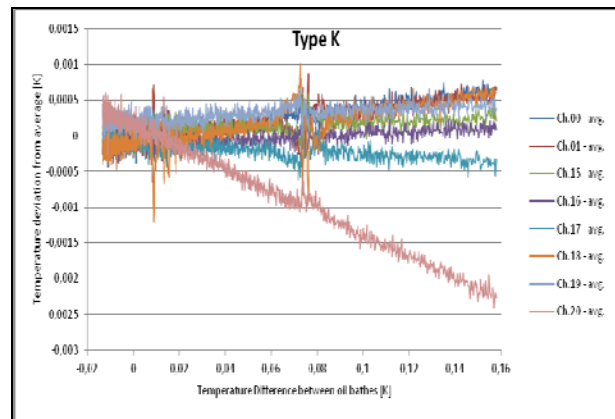


Figure 32: Characteristic curves of all welded type K thermocouples over about 0.2 K

Due to the low signal level, electromagnetic pulses can degrade the measurements. While the system has successfully be implemented in comparators with linear driven motors at PTB and the collaborator SIOS, a pulse width modulated motor increases the measurement noise by a factor of about 7. The same behavior could be seen at a precision milling machine. This sensitivity against environmental influences will make a widespread use of thermocouples not very probable. The small signal level also has shown some limitations in the use of control loops due to the necessary time for signal averaging.. Specific work is necessary to develop appropriate shielding of the sensor from the electronics for critical environments.

3.4.4. Conclusion and outlook

A temperature measurement system was developed that incorporated multiple measurement sensors, with both platinum resistance thermometers and thermocouples. The performance of 32 thermocouples, made from different materials and from different manufacturers, was tested, including the effects of stress, motion and heat on their behavior. The temperature measurement system was verified to be accurate to the sub-millikelvin (mK) range (one thousandths of a degree Celsius).

A room-temperature calibration device was developed using materials that melt at known fixed points – water at 0.01 °C and gallium at 29.76 °C. A range of different gallium-alloys were investigated to find the optimal compound. To validate the performance of the calibration device, were investigated over a period of 18 months, and compared with a 4th cell which was newly manufactured. All four cells produced results that agreed to within ± 4 mK.

The objective was achieved, as the room-temperature, self-calibrating measurement system was successfully developed. The system was then further enhanced to act as an active temperature control system for precision engineering equipment, capable of reducing heat flow through equipment to maintain its stability. Control software was developed for the thermocouples, and different types of control algorithms, including PID and Model Prediction Control, have been implemented. Using a preamplifier developed at PTB, an uncertainty level of 0.2 mK_{pp} can be reached at measurement times of below two seconds, approximately a thousand-fold improvement compared to a nanovolt meter.

3.5. Objective 5: Development of improved thermal modelling

3.5.1. Introduction

Thermal modeling allows thermal design to be optimized for example by optimizing material selection and placement of heat generating devices. For the modeling it is often advantageous to use a reduced model, which requires less computation time and allows modeling more easily the behavior of control loops for active tempering. The Model Identification Method (MIM), which has been developed by the unfunded partner PPRIME will be used. The MIM modeling has been verified by the TU Ilmenau in the project by comparison with FEM calculations and on an idealized artefact in vacuum by analytical calculations and measurements.

In this project thermal modeling is exemplarily used to calculate the behavior of the metrology frame of a form measurement device at LNE and to optimize the design of a new type of cooling element for a camera of a high resolution microscope used in a length comparator at PTB.

3.5.2. Modeling of a cylindricity measuring machine

This study could not be performed on the machine itself, so a special setup reproducing the metrology loop was built as shown in figure 33. All the modeling and experimental studies have been done on this setup. From this modeling we built a reduced model using MIM (Model Identification Method) technique that reproduced the thermal behavior of the setup with a limited numbers of inputs in order to be able to build a control system to regulate the temperature at the critical points of the setup.

The MIM consists in three main steps:

- 1) Define the structure of the Low Order Model (LOM) equations able to adequately describe the involved physics,
- 2) Generate some input-output data representative of the system dynamics. Those data come from in-situ measurements or from numerical simulations,
- 3) Identify the parameters of the LOM equations through the minimization of a functional based on the quadratic residuals between the previously generated output data of the system on the one hand and the outputs of the LOM on the other hand, for the same input data.
- 4) The MIM therefore aims to adjust the LOM constitutive parameters using optimization techniques, in order for the LOM to mimic the data characterizing the input-output dynamics of the system.

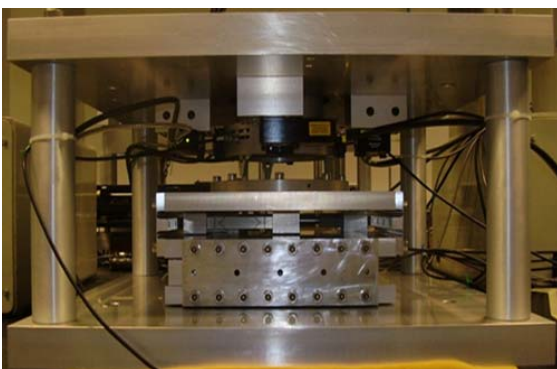


Figure 33 : *Experimental set-up*

In a first step, a study of the thermal behaviour of the setup has been done using finite elements method (FEM). For this study we have focused our interest on the temperature of 8 points close the metrology frame of the setup since it's the most critical part to obtain the lowest uncertainties. In a second step we wanted to be able the reproduce the results from the FEM but with a limited set of parameters (less than 10) in order to be able afterwards to develop a control that will stabilize the temperature in the region of interest: the metrology frame.

We first modeled the setup assuming that the 4 laser interferometer heads were the principal perturbations of the setup (1,2 W heating power per interferometer head).

This model was then reduce applying MIM, to a 10 inputs model reproducing FEM results with differences in temperature lower than 10 mK (Figure 34).

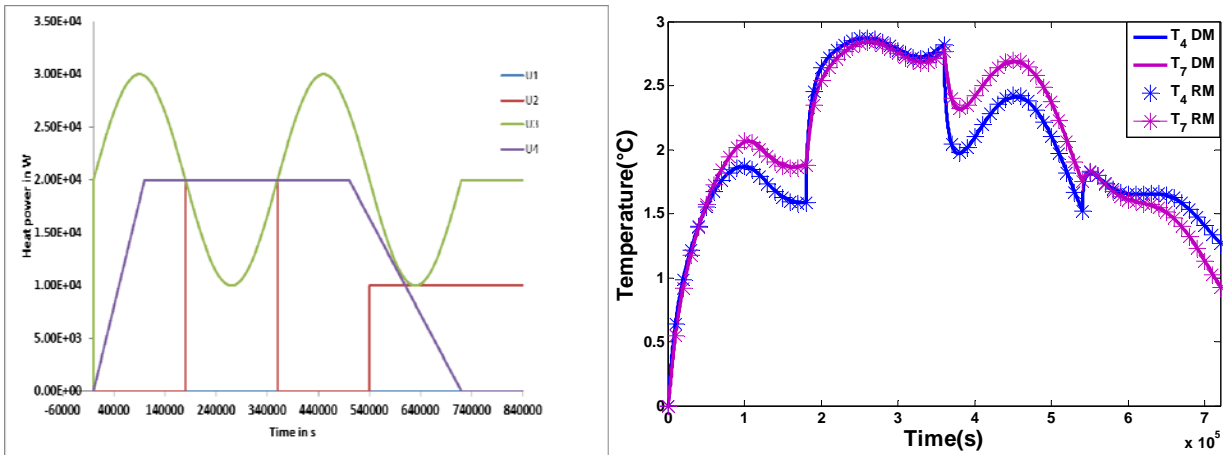


Figure 34 : (a) heat power applied, (b) Temperature evolution in 2 points, comparison FEM calculations (lines) and MIM results (stars).

Using this reduced model, numerical simulations have been performed in order to compare both control methods: Linear Quadratic Gaussian (LQG) Compensator and Model Predictive Control (MPC). The Linear Quadratic Gaussian control is applied to systems with noisy and unmeasured states. It relies on the separation principle stating that the optimal control solution is divided into two parts: Linear Quadratic Regulator (LQR) and Linear Quadratic Estimator (LQE) also known as Kálmán filter. Model Predictive Control is one of the most popular control methods based on optimal control strategy. Its principle relies on the use of a model of the system to predict the plant’s behavior and then choose the best control in the sense of some cost function within certain constraints. The future response of the controlled plant is predicted over a prediction horizon. These simulations showed that both methods have similar performances, but if we want to increase the performance MPC works fine provided that the number of time steps for prediction horizon is sufficiently large, for LQG there is a threshold value where control fails. Based on these results PTB selected the MPC algorithm as standard in the temperature measurement and control electronics.

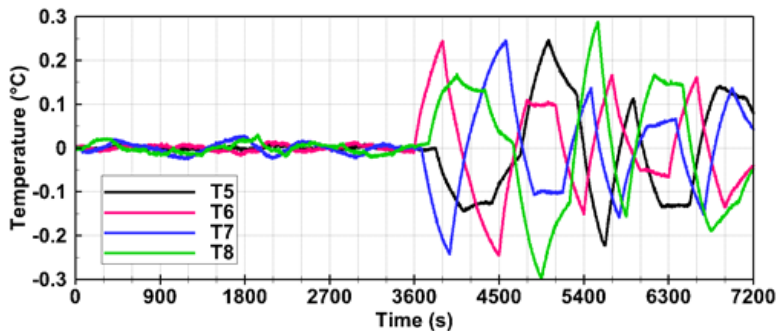


Figure 35: Example of the effect of the simulated control (here MPC) on 4 temperatures. During the first hour the control was ON then he was switched OFF. The “zero” line represent the target value. The standard deviation of the temperatures with the control ON is 4 mK.

We developed tools and we build a reduced model based on our assumption (the 4 laser interferometer heads as main perturbation) and FEM calculations.

During the second part of this project, we worked on real temperature measurements. After this, we have measured experimentally the temperature in 19points of the setup using calibrated Pt100 sensors in order to see if the temperatures when switching the laser interferometer ON (Figure 35).

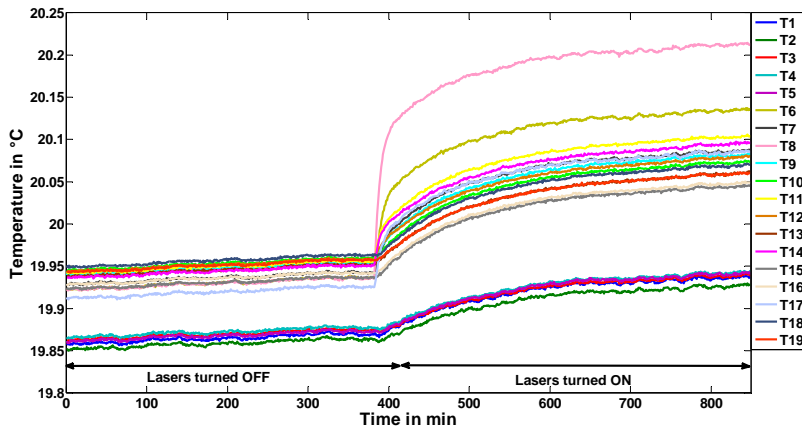


Figure 36: Temperature measurements

temperatures in the 19 points increase. We can however see that the increases of the temperatures that are close to the laser interferometer L1 are more important. This means that the power dissipated by the laser L1 is higher. After 6 hours, we can see that all the temperatures reach a steady state. Therefore, since measurements on the real machine will be performed long after that interferometers will be switched on, they cannot be considered as a perturbation in our system. A comparison of the modeling for different laser power and experimental results allowed us to estimate the real dissipated power: 1.5 W for one laser and 0.65 W for the others.

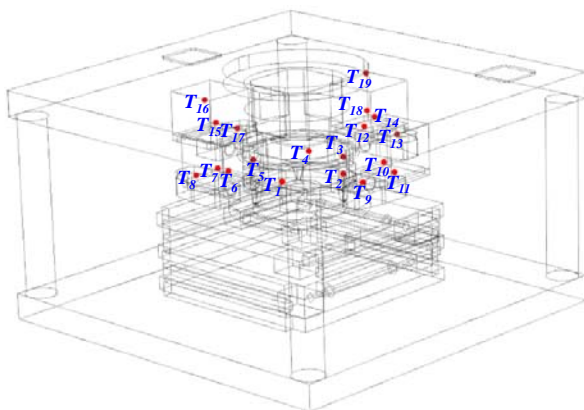


Figure 37: CAD of the setup with the position of the 19 pt100 temperature sensors

A new model was needed, using as perturbations, the heat coming from the guiding slides and also the ambient temperature. We added 3 heating wire to simulate the guiding slides and 4 Pt100 sensors to measure the ambient temperature around the setup, we kept the 19 PT100 close to the region of interest (metrology frame) Figure 37. An extensive study of the thermal effects on measurements, calibration procedure and cylindricity measurements using time dependant FEM calculations was done.

The cylindricity measurement corresponds to the combination of roundness measurements at several height levels and vertical translations. The roundness can be measured one or several times successively to provide redundant data and thereby more accurate information.

Two simulations were performed for two signals composed of 11 successive steps of 0.5 and 1 W magnitude. The power of 0.5 W corresponds to the analytical estimation of the power dissipated by the ball bearing spindle generating the rotational movement, while 1 W represents the estimated power dissipated by the linear mechanical guiding system generating the vertical motion.

The first simulation was carried-out over a simulation time of three hours, which corresponds to several roundness measurements at each level. The resulting temperatures $T_{1..19}(t)$ evolutions are shown in Figure 38. The results show a maximal temperature increase of 0.12 °C between the beginning of the simulation and its end. One can also notice that this heating does not create inhomogeneous temperature field in the metrology frame.

The second simulation was performed with shorter duration, which corresponds to the cylindricity measurement case where only two roundness measurements are assessed for each level. The vertical translation of the metrology frame duration is estimated to 30 s while the two rotations of the cylindrical artifact (simulating two roundness measurements) duration are estimated to 60 s. The results show that the evolution of the temperature is quasi-linear. Its variation is less than 0.02 °C for the entire time span.

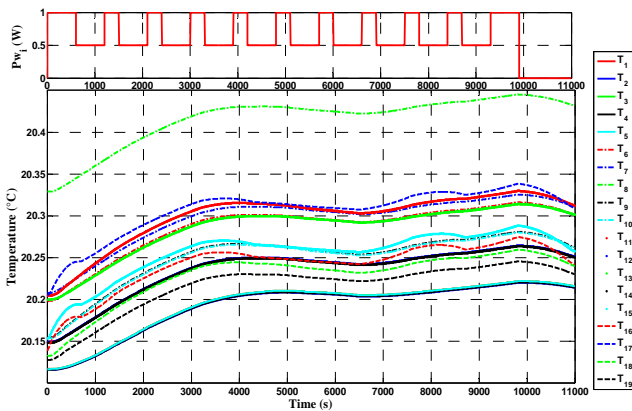


Figure 38: time-dependent FEM simulation of the temperature when combining translations and rotations (cylindricity assessment simulation). The input powers generated by the 3 heating wires follow an incremental signal varying between 0.5 and 1 W.

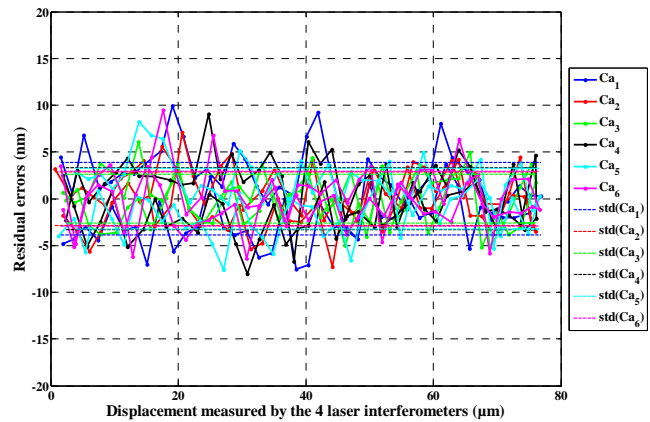


Figure 39: Experiment set-up with the aluminium shields, The input powers amplitudes generated by the 3 heating wires $P_{W1,2,3}(t)$ follow an incremental law varying within 0.5 W and 1 W (simulating a cylindricity measurement); evaluation of the residual errors of the capacitive probe C_1 for 6 calibration procedures $Ca_1, Ca_2, Ca_3, Ca_4, Ca_5$ and Ca_6

So if one do the measurements in a reasonable amount of time (less than 20 min); thermal effects will be limited (drift < 0,02°C) and no special action (control) will be needed. This study revealed also that the temperature distribution in the metrology frame are less than 0.01 °C whatever the selected conditions. Even if the external input power causes the temperatures $T_{C=1..19}(t)$ increases in the set-up, the temperature distribution in the metrology frame remains constant along the test duration and the observed temperature fluctuations are less than 0.003 °C. Other functions of the machine have been investigated, like in-situ calibration of the capacitive sensor vs. laser interferometers (Figure 39). For power around 1 W the effects on calibrations are limited.

In conclusion all these investigations showed that thermal effects in a good environment like our laboratories have a limited impact on the machine performances. Therefore the need of a control implementation is not urgently needed, and it was not implemented. This possibility will be kept for future improvements of the machine.

3.3.3. Cooling approaches

In order to reduce the temperature gradients in a measuring microscope of the PTB nanometer comparator, which are generated by a CCD camera, a cooling of the camera must be implemented. The thermal image of the camera is shown in Figure 40.

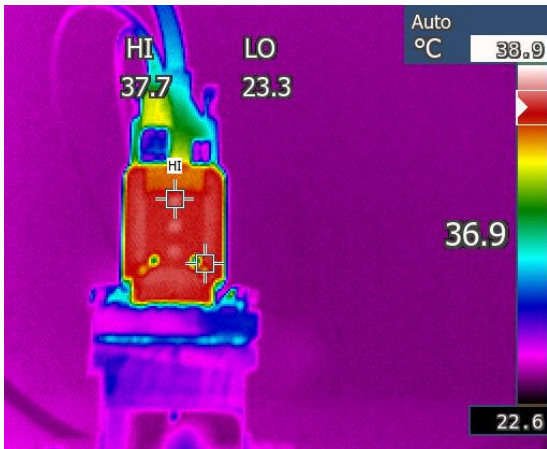


Figure 40 Thermal image of UV-camera cooling elements will not be used.

For cooling, one can generally distinguish two approaches:

Active cooling; In active cooling approaches actively servo-controlled heat sources or heat sinks are used to control or stabilise the temperature of a component or an instrument. Typical sources or sinks which are utilised are e.g. peltier elements or electrical heaters. Typically, they are applied in combination with heat exchangers to temper working media like gases or fluids, which exchange the heat with the components to be stabilized in temperature. Active cooling approaches offer advantages as the temperature at the position of interest can be controlled directly. But, applied to precision dimensional measurement instrumentation they also have drawbacks. The moving working fluids in pipes or even ventilating air can be a source of disturbing vibrations. Therefore active

Passive cooling; Constructive changes in instruments which are made to optimise the paths of heat flow or to minimise the thermal sensitivity of the set-up are summarised in the category "passive cooling". Here, by means of constructive changes the parasitic heat is guided away to the environment. Due to usually minor cooling power compared to active approaches, the resulting temperatures are depending on the boundary conditions and the temperature deviations will not become zero.

The starting point of a thermal optimisation is a sufficient understanding of the heat transport phenomena or temperature fields in the instrumentation. The boundary conditions for this are as follows: The camera has an installed electrical power of $P \approx 4,5W$, which is mostly transformed to parasitic heat during operation. The Nanometer Comparator and measuring microscope are used in a temperature stabilised chamber at $T_{amb} = 20 \text{ °C}$. In this chamber air continuously flows from the ceiling to the bottom with $v_{air} = 0.2 - 0.4 \text{ m/s}$. Generally, this air flow could be used to cool down the microscope and camera with a fin cooler which is mounted at the camera. Nevertheless, the camera still heats up significantly as can be seen in Figure 41 from a FEM model.

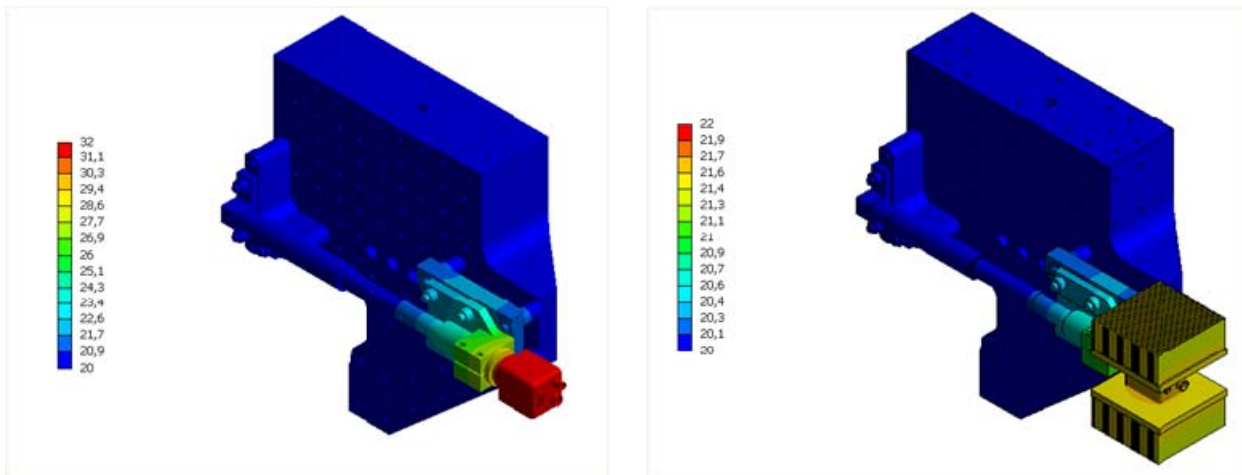


Figure 41 Simulated temperature field in measuring microscope and camera (left) and camera with fin coolers (right)

In this FEM model without cooler, the maximum temperature of the camera was about 34°C which is close to the temperatures that were measured previously by thermal imaging (Figure 40). Furthermore, it can be seen in the simulated temperature field, that some parts of the microscope heat up significantly due to the heat transport by thermal conduction along the Invar mounting elements.

To reduce the camera temperature and the heat flow into the instrument to least possible values, one may attach additional cooling elements to the camera. With that, the temperature distribution can be homogenized, as can be seen in Figure 41 (right). But, due to the finite thermal resistance of the cooling

elements and the camera and the limited heat transfer coefficient of slow moving air, significant temperature gradients in the microscope and the mounting elements remain.

A new method for a passive cooling was developed by TU Ilmenau. Here, the inverse principle of a fixed-point cell which is normally used for the calibration of thermometers is applied in the cooling set-up [7]. Most of the fixed-point cells consist of a cylindrical crucible which is filled with a material of which the temperature of the melting point T_{ph} is precisely known (Figure 42, left). When a calibration of thermometer by means of such a cell is performed, the thermometer is inserted into it and heated up together with the cell using an external heat source. When the exterior temperature T_1 reaches the melting temperature T_{ph} of the fixed-point material, its melting starts and the material absorbs the externally introduced heat and transforms it into the latent heat of melting until the material is molten. The inverse principle of a fixed-point cell can be used for passive thermal stabilization of an instrument. Here, the heat source is encased by the cell and therefore is surrounded by the material which changes its phase (Phase Change Material - PCM). When the source is switched on, the PCM starts to melt and absorbs the generated parasitic heat. As long as the melting of the PCM takes place, a thermal equilibrium is present in which the exterior of the cell remains below the melting temperature and therefore shields the source of parasitic heat from surrounding thermally sensitive parts. The PCMs latent heat of melting is used as a heat sink. To keep the temperature of the shield as close as possible to ambient temperature, a PCM with a melting temperature slightly above 20 °C had to be chosen. Depending on the material, the melting procedure develops in different ways. This materials have been investigated by the PTB for the use as a fixed point cell as described below, where also the melting curve is sketched.

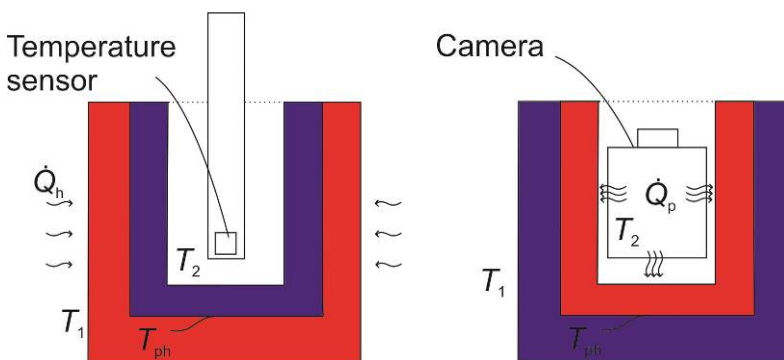


Figure 42: Working principle of a fixed-point cell (left) and the PCM-cooler (right)

To prove the principle of a PCM-shielding of the camera, a demonstration model including a PCM-container and a camera was designed and developed using thermal Finite-Element-Analysis (FEA). In this model, the camera is surrounded by a container made of polyethylene which shields the camera at four sides. The cavity of the container is filled with the PCM. At the back of the camera a cooler is mounted which

additionally cools down the camera. The camera itself is fixed by mounting elements. For testing purposes, the whole assembly is mounted on a base plate. Figure 43 shows the CAD model and a picture of the prototype. The aim of the design is to reduce the heat flow into the measuring microscope and the Nanometer Comparator as well as to provide a more stable temperature environment for the camera. To reduce the heat flow into the comparator, the mounting elements are manufactured from materials with a low thermal conductivity as Zerodur.

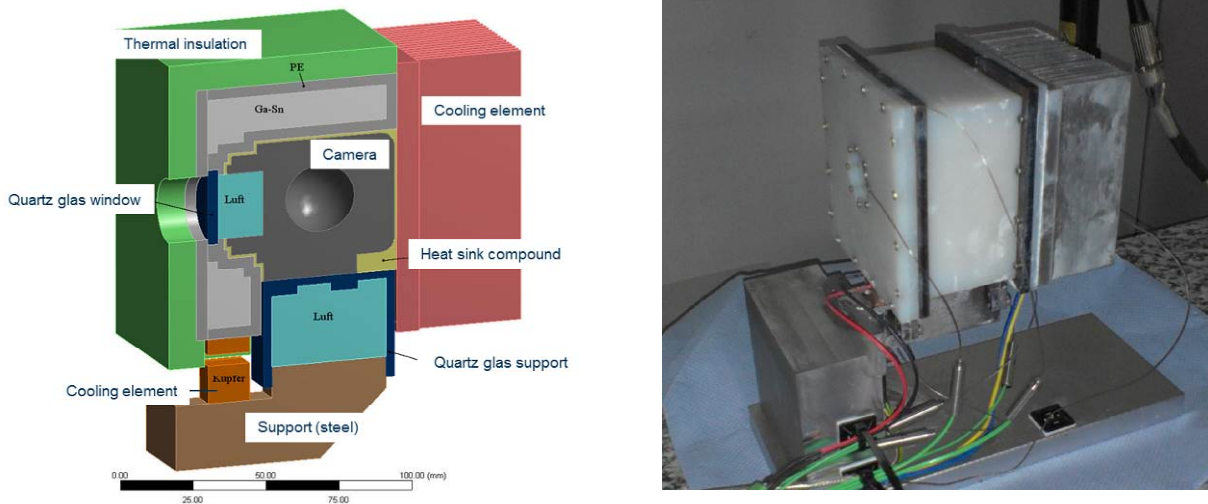


Figure 43: Design of demonstration model for PCM-Shielding

The theoretical behavior of the design was investigated in thermal calculations using FEA. In these dynamic simulations, where the camera was switched on at time $t = 0$ s, the time dependence of the temperature distribution was estimated. Results of this simulation are shown in figure 44. It can be seen, that for $t = 0$ s no heat sources influence the set-up and therefore the temperature is homogeneous at $T_{ph} = 20$ °C. When the heating power is applied to the camera, the camera and the fin cooler start to heat up ($t = 0.5$ h). But, due to the absorption of the parasitic heat by the PCM the exterior walls and mounting elements remain cold for several hours. After approximately 7 to 9 hours, the PCM is already molten in some areas and the quality of the thermal shielding decreases. After approximately ten hours, all PCM is molten by the cameras parasitic heat. The calculations show that it is possible to provide a thermal shield, a cold exterior surface and stable thermal conditions at the mounting for up to 8 hours. This is shown in figure 44. After that, the PCM must be refreshed or solidified again. This fits very well to the measurement cycles of the comparator, where some time is necessary to wait after adjustment until a thermal equilibrium in the whole machine is reached.

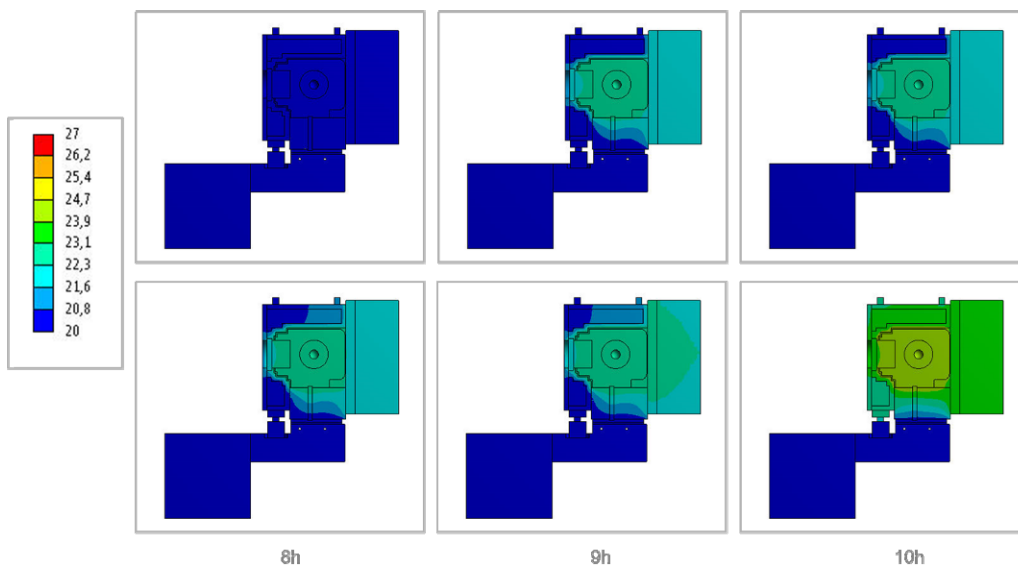


Figure 44: Temperature distribution in the demonstration model calculated by means of FEA

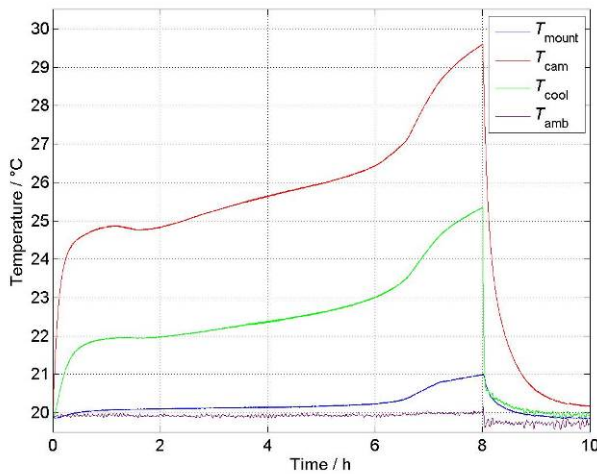


Figure 45: Results of a measurement in a climatic chamber

The FEA Analysis was verified by the demonstration model. For the measurements, it was placed in a climatic chamber and was measured at the same conditions as it was assumed for the calculation. The temperature at certain points was monitored by means of thin mineral-insulated thermocouples, which allow a measurement without self-heating effect of the sensor. In the graph in figure 45, three typical periods of the phase change can be observed. In period 1 up to one hour, the set-up heats up and thermally stabilises. Between 1 h and 7 h, quite stable thermal conditions are present. In period 3 after approximately 7 hours the PCM is nearly molten and the temperature starts to increase significantly. The measurements agree quite well with the calculations and show, that a thermal shielding and stabilisation of the camera can be achieved by PCM-Shielding.

3.5.4. Conclusions

The project developed reduced thermal models that incorporated only the variables that were found to significantly affect the flow of heat. The model was verified through: 1) a comparison to results from finite element analysis, and 2) experimentally, using a simplified demonstrator setup. The successful modelling approach and results have been reported in a best practice guide. The models were then used to develop control algorithms to increase temperature stability of a form measurement machine and for the optimized placement of cooling elements for a line scale comparator.

As a case study, a novel cooling system was developed for a camera in an ultraviolet microscope, based on a passive cooling method developed by the Ilmenau University of Technology in Germany. The cooling system improved the microscope's stability, and the accuracy of the length measurements the microscope is used to make. A prototype of the cooling device was produced, and verified through modelling. By implementing the improved temperature measurement electronics at the PTB length comparator, combined with the new cooling element for the microscope camera, the measurement uncertainty was successfully reduced. This reduction helps meet customer demands for the calibration of length scales with the highest worldwide accuracy.

3.6. Objective 6: Setup of a database for measurement results of the JRP with information on stability, thermal dilatation and hardness of material samples, joint structures, sensors and actors.

The project has generated and collected data on material and joint performance under various environmental fluctuations, and under time variation from weeks to months as described in the Sections 3.2 and 3.3. Measurements have covered dimensional, surface (hardness and creep) and thermal variations. These results have been published to support the design of optimised precision tools, industrial equipment, and standards for reference materials. All measurement results: drift rates, CTE, hardness and creep from material samples or joints generated or measured in the project are available in a [publically available database](http://projects.npl.co.uk/T3D/publications.html), which can be found under <http://projects.npl.co.uk/T3D/publications.html>. The project partners will continue to update with non-confidential measurement results. The database is also open for new contributors, who can supply data for long time stability, coefficients of thermal expansion, hardness and creep of materials and joints.

3.7. Objective 7: Good Practice Guide for developing temperature insensitive precision engineering measurement and tool machines.

Good Practice Guides based on the project's results have been published on the project website, in the [EURAMET Publications Repository](#), and have been partly published in journals. These guides will help improve the control of production processes, contributing to more efficient, safe and reliable precision engineering. The good practice guides have been derived from the results and the experiences of the scientific work in the project.

From the work regarding the high resolution heterodyne interferometer developed by VSL with support from PTB the good practice guide "Measurement of relative length changes in sample up to 50mm with picometre uncertainty over durations up to 1 week" has been derived. More detailed results are described in chapter 3.1.2. New results from the integration of the interferometer in a vacuum chamber, which will be done after the project end, will be later published.

NPL has described the methods developed to allow for traceable indentation at elevated temperatures in a guide "traceable calibration of instrumented *Indentation Instruments* as a function of temperature". More detailed description of the verification measurements can be found in chapter 3.2.2. This guide also includes the measurement uncertainty budget, which can be used as a pattern for users.

After developing methods to glue two gauge blocks keeping parallelity, PTB as an example has optimized the glueing process to minimize the long time drift and tilt of the connection. Every new glueing process was investigated in the gauge block interferometer. The soldered samples from FHG were initially already very stable, so that no optimization was necessary. This results are in more detail discussed in chapter 3.3.3. This process is also described in a good practice guide about "Thermal optimizations of joints".

Three good practice guides has been derived from the work regarding the thermal optimization of machine tools. The basic method for the optimization is the thermal modelling. The computing intensive but universal finite element method has been compared with a reduced model after the MIM method. In the good practice guide "Thermal modelling of precision engineering equipment" the application of this methods is described.

The reduced modeling was used as a basic tool for finding good locations for cooling elements as well as for model based control of coolers and heaters. Additionally the method was applied to find optimized solutions for the design of the measurement circle of a roundness measurement machine. The application of the method has been described in the two good practice guides "Locating and control cooling devices on thermal sensitive instruments" and "Developing instruments with minimal thermal sensitivity".

4 Actual and potential impact

4.1 Dissemination

Stakeholder interaction

The results of the project are mainly of interest for tool manufacturers in the ultra precision engineering. This are, especially at the moment, companies involved in the supply chain for semiconductor lithography. Many of these companies in Europe are in the list of the stakeholders of this project. Therefore the most important dissemination is achieved by direct contact with the stakeholders. In addition to meetings at conferences and visits in various institutes, presentations have been given in most of the stakeholder companies. After the end of the project all partners will give presentations at the stakeholder companies in their countries about the final results of the project.

Conferences

For Precision Engineering in Europe, the EUSPEN conferences are key events. The project goals have been presented at the start phase of the project in Stockholm 2012. The final results have been presented at the meeting of the EUSPEN special interest group at Zürich 2014 and in a workshop attached to the EUSPEN conference 2014 in Dubrovnik. In between, different aspects of the project have been presented at general conferences like the TEMPMEKO as well as on more specialized and industrial targeted conferences like the Institute of Physics Meeting on Nanoindentation in London and workshops organized by companies like

Schlumberger in Cambridge and Bosch in Stuttgart. Overall, twenty-one presentations have been given and additional five posters have been presented. Further presentations after the end of the project are already fixed.

Workshops

The EUSPEN council made it possible to attach the project workshop to the EUSPEN conference 2014 in Dubrovnik. At the last day of the conference all project partners presented the results of the project to 50 participants mainly from industry.

A second workshop has been included in the 58th International Scientific Workshop IWK in Ilmenau. As this conference had several parallel sessions, the number of 25 participants was lower than in Dubrovnik.

NPL organised annual industrial advisory group meetings at their laboratories in Teddington to disseminate project results and maintain industrial input in the project. Each IAG meeting attracted between 20 and 40 industrial participants.

Standards

NPL has disseminated the results of the project to both ISO/TC61 on the measurement of hardness in plastics and ISO/TC164 which develops standards on the mechanical properties and hardness of metals. The project delegates to these meetings have assisted in the liaison between these two standards committees, ensuring consistent standards are developed in both fields. ISO/TC164 has been involved in developing the main standards for the use of nanoindentation, whereas ISO/TC61 has assisted in the development of standards specific to the micro/nano hardness testing of plastics.

PTB has presented project results in the subcommittee SC9 of the ISO TC 201, which works on standardization of AFM metrology. This information was especially targeted to a subgroup, which discusses thermal influences on AFM measurements.

Publications

One important output is the technical knowledge from the work in the project, which has been carried out. This knowledge was published so that it can be used by interested scientist and technicians

Overall, 12 peer reviewed papers have been submitted to journals and conference proceedings in precision engineering and temperature related publications.

Other dissemination

Project results have been presented in different house journals and annual reports of the institutes involved in the project.

One publication has been successfully submitted to a trade journal. A second submission to various journals failed as the topics of this project do not currently fit to the more general mechanical engineering oriented journals. Results of the project have also been presented at three exhibitions

To allow dissemination of the project results to the European metrology institutes, a presentation at a EURAMT TCL meeting has been given. Also regular in house workshops have been used to spread information on the project in the metrology institutes itself.

The gained knowledge of different parts of the project is conditioned into Good Practice Guides for information of interested users, which are listed under publication list.

In order to improve the dimensional and thermal stability of ultra precision engineering measurement and production tools, properties, like aging, drift and thermal dilatation, of materials and joints needed to be gathered in the project. Unfortunately, this information is not commonly accessible to small or medium-sized businesses. One reason is that literature focuses rather on the mechanical stability or other characteristics of joints, but not on dimensional stability. Suppliers of adhesives, screws etc. often provide no or even misleading information about dimensional stability. Therefore a database which can be found under <http://projects.npl.co.uk/T3D/publications.html> has been set up to provide public access to data gathered in the project. This database will be further supported by adding publicly available measurement results from the institutes.

4.3 Direct project uptakes

The Fraunhofer IOF in Jena, was acting as a unfunded partner and an example of a company that is in need of appropriate measurements on their products. The IOF has developed and refined specialized, inorganic joining techniques such as silicatic bonding, AuSn laser-based thin-film soldering and Solderjet Bumping. The technology has been established and improved over the past years in order to assemble optical components for ultrahigh-precision instruments. The IOF has developed samples appropriate to the instrumentation used in the project. These joining techniques were characterized on the basis of absolute length measurements performed at PTB in a time period of over a year and a temperature range between 10 °C and 40 °C and regarding short term stability at VSL. Other samples were provided for creep measurements at NPL. These measurements performed in the project shows, that soldering of optical components can be used for long time stable adjustments. The IOF can use that results for gaining wider customer interest for this technology.

Moreover, the results of the stability measurements have impacted in-house assembly of silicon parts at VSL of a micro gravitation measurement device where drift issues are critical. The Picodrift instrument has also been used for the calibration of a virtual reference standard as required/developed for the 7th framework programme project "Aim4NP".

MicroMaterials the manufacture of NanoTest instruments has shown considerable interest in the project becoming a collaborator during the project and providing NPL with access to additional test equipment. The procedures developed during the project to monitor and control specimen and indenter temperatures are being considered by MicroMaterials as an alternative method for their instruments.

The investigations of temperature fix points using eutectic alloys clarified the limits for the calibration or validation of temperature sensors. This will help to avoid further research activities and developments in the wrong direction. Due to the physical limits the use of such a fixed point looks not very promising, as it is proven that some temperature sensors can provide this stability for some years without recalibration.

The thermocouple temperature measurement system have for some months been tested in a Nano positioning and measurement machine at SIOS in Ilmenau. The company is thinking about the use of the instrument. But due to the influence of electromagnetic distortions, it is not simply possible to use it in arbitrary environments. Therefore, more investigations on better shielding must be performed first before this can be decided.

The long term investigation of thermocouples was able to confirm the assumption, that thermocouples can be used over small measurement ranges without recalibration. By measurement of the scatter of the individual sensitivity, the measurement uncertainty in dependence of the measurement range could be estimated. Due to these results two small companies will commercialize the temperature measurement system. Magnicon is selling the low noise preamplifier developed at PTB. The first application was its use in a squid based current comparator. Magnicon will do the adaption of the relay switching unit to this system. The preamplifier needs a high amount of adjustment work, which will end up in high cost, so that this system will only be used for special applications with very high demand regarding temperature measurement uncertainty. For applications with lower demand in measurement uncertainty, the cheaper system based on the nanovoltmeter will be further used. The startup company MPRO will take over this standard system. Before they can sell it as a product, the relay switching box has to be redesigned, as the previously used relays are not available anymore. It is in discussion to extend the system for the use of thermistors. The software is already prepared for this type of sensors.

4.4 New Measurement services by the NMIs

The central aim of this project is the high precision measurement of thermal dilatation, dimensional drift and creep. The instrumentation used is very sophisticated and complicated to operate. Therefore it is for companies not very attractive to obtain an own measurement setup, as the companies, even large ones, do not have continuous demand for such instrumentation. Therefore metrology institutes like PTB, NPL and VSL are offering these measurements as a service for the European industry. The intention of this project was mainly focused on the deployment and improvement of new services at the metrology institutes. Despite some direct uptakes of project results have been generated during the project or are arranged for the near

future. Some new services directly depend on the work in this project. As already mentioned, this in the first place services for the measurement of thermal dilatation or dimensional stability not only for material samples but also for joints, sensors and actuators can be supplied.

PTB could successfully demonstrate that by gluing and screwing of gauge blocks the parallelity could be maintained. The parts have been glued under control in an interferometer especially set up for the project. The Fraunhofer IOF has demonstrated that it was possible to keep the parallelism also during soldering processes and have additionally supplied the project with glass ceramic samples connected by anionic bonding. An important finding during the measurement of adhesive joints, is the importance of not only considering thermal influences on stability (thermal expansion and thermally-induced drift) but, as not surprising, also the impact of humidity as an additional source of drift. As the PTB interference comparator is located in a vacuum chamber, the humidity and gas compositions can easily be adjusted for more specialized investigations. Due to the experience from this project PTB can supply various interferometric measurements for joints, sensors and actors including the preparation of the samples by gluing, or adjustment of screwed connections. The support in the sample preparations will allow also smaller companies to use this service. Fur European companies have expressed interest in stability measurements at PTB.

By using a heterodyne detection scheme the interferometer at the VSL picodrift instrument, very high resolution measurements in the range of 10 pm is possible. After improving the environmental conditions, very sensitive measurements of short term stabilities will be possible. To demonstrate an example of a measurement service using the picodrift instrument, The high-resolution interferometer at the VSL picodrift instrument will be used in the near future in cooperation with the PTB and the IMMS GmbH to perform some basic investigations on interferometry for the improvement of position measurements for stage motions for an customer of IMMS. We have to wait at the moment on the delivery of some custom made optics. At NPL the results of the project will allow to perform indentation measurements with lower uncertainties and also for an increased temperature range as a new service.

The Model Identification Method (MIM) developed by the project partner PPRIME has been successfully verified for precision engineering applications in collaboration with LNE and the TU Ilmenau. It was used to optimize a cylindricity measurement tool at LNE by optimizing the place of the heat sources in the instrument and for a better placement of the instrument. LNE can provide now measurements with the thermally optimized cylindricity comparator with lower uncertainty.

A new type of cooling element was developed by the TU Ilmenau. Using the fixed point material as a thermal shield around heat sources, a heat flow into machine structures can be blocked. The melting process can last 8 hours or longer, dependent on the amount of material and the generated heat, until the phase changing material has melted. This method is easy to apply and no moving parts or fluids are necessary, which could generate vibrations. By implementing the new cooling element for the CCD camera of the measurement microscope at the PTB length comparator, the measurement uncertainty at this comparator will be reduced. Together with other changes this will help to meet customer demands in the calibration of lithography masks for the manufacturing of semiconductor devices. This method will not be universally applicable, as a specific amount of time is necessary to freeze the phase changing material after the melting process. Therefore no 24 hour operation is possible. But it fits well with the use of reference measurement tools, where after adjustment of the samples by the operator, some time will be necessary anyhow until the thermal equilibrium is reached.

The improvement of the thermocouple metrology will also help to reach the necessary uncertainties of the determination of the Avogadro constant using a silicon sphere. As silicon has a relative large dilatation of about $2.5 \cdot 10^{-6} \text{ K}^{-1}$ a temperature uncertainty of better than 1 mK is required for the temperature field around the samples in vacuum. By determination of the Avogadro constant a new definition of the base unit kg will be possible.

4.5 Scientific outlook and future impact

Based on the results and experience during the work, further improvements beyond the scope of this project will follow.

Procedures have been developed for the high temperature calibration of nanoindentation equipment, enabling: displacement, force, frame compliance, indenter geometry and specimen temperature to be calibrated at elevated temperatures. Two candidate reference materials have been proposed that are stable at elevated temperatures for the calibration of frame compliance and indenter geometry using the two reference material method. Arrhenius analysis of creep data obtained from the nanoindenter has also demonstrated the potential of using the instrument for conducting accelerated creep tests at elevated temperatures and relating these back to long-term ambient temperature service conditions.

Another potential impact is the measurement of the dimensional and thermal stability of more “exotic” materials. The most precise length measurements are carried out with interferometers as described above, where the parallel end faces of the samples are required to have optical quality. For high-precision thermal expansion measurements (especially in the cryogenic range) of some materials used in space, like SiC, it is feasible to polish to optical quality and contact to a base platen by wringing, which stability is proven over a large time frame. However, for other materials of interest (e.g. Invar, CFRP) this optical surface finish may not be that easy or even impossible to achieve. Well investigated adhesive joints could be used to contact a gauge block or mirror plate to the front face of a (rough) sample surface and possibly also to mount a sample with its bottom face onto a platen. Both, the thickness of the adhesive layer and the resulting tilt angle of the bonded mirror have to be minimized. We have produced adhesive layers of far below 1 μm thickness and demonstrated the provisions to guarantee a negligible influence on CTE.

As the optical interferometers require cooperative and parallel surfaces at the samples to measure thermal dilatation, not all type of samples are usable. Partly that problem can be solved by gluing mirrors onto the parts as described earlier, but some times the cost for the special manufacturing is too high or the sample may not be damaged. For these cases an idea has been developed to use a flexure hinge to generate a tactile probing of the sample, while pushing the sample against a reference plate. The probing element and the reference plate providing mirrors for the interferometer. With an initial measurement of the dilatation of the mirror, this effect can be subtracted later. We assume that the mechanical probing will increase the measurement uncertainty by an order of magnitude. Additionally it allows using high resolution interferometry for creep measurements similarly like indentation tools.

Regarding temperature measurements with thermocouples further effort will be done to overcome the above mentioned limitations. Some work on the effective shielding of the thermocouples will be done, to allow for a more widespread use. A combination of thermocouples with small thermistors will be investigated to allow for a high dynamic measurement with the very sensitive thermistors and a continuous drift correction by the thermocouples. A combination of the sensors aims to improve the differential temperature control of flowing gases and liquids.

References

- [1] “Roadmap Precisiechnologie”, Innovation-driven research program (IOP) on precision technology, SenterNovem, www.senternovem.nl, Utrecht, The Netherlands, 22 January 2004
- [2] European Technology Platform EuMaT European Technology Platform for Advanced Engineering Materials and Technologies (2006), ftp://ftp.cordis.europa.eu/pub/technology-platforms/docs/eumat-roadmap-ver27b-kj-08062006_en.pdf, in particular comments on thermal expansion behaviour, e.g. on p. 62 (composite materials), p. 30 (multi-material (hybrid) systems), p.38 (modelling)
- [3] European Space Technology Platform Strategic Research Agenda V1.0 (2006) <http://cordis.europa.eu/technology-platforms/pdf/estp.pdf>, in particular section on Structures & Thermal Control, p. 74ff
- [4] ISO/TC 164 Business Plan “Mechanical Testing of Metals”, 2004.
- [5] International Technology Roadmap for Semiconductors ITRS <http://public.itrs.net/Links/2009ITRS/Home2009.htm>, see e.g. p. 14 of the lithography part of the ITRS stating ‘Equilibrium and non-equilibrium models of thermal effects are also essential for designing exposure tools’

[6] Ueda S., Kameyama T., Matsunaga, T., Kitazono K., and Saechiques, E. "Re-examination of creep behaviour of high purity aluminium at low temperature" Journal of Physics: Conference series 240, 012073, 2010

[7] M. Schalles, F. Bernhard, Triple-fixed-point blackbody for the calibration of radiation thermometers, International Journal of Thermophysics 28 (6) (2007) 2049{2058.

[8] Bönsch, G., Schuster, H.J., Schödel, R.: Hochgenaue Temperaturmessung mit Thermoelementen (High-precision temperature measurements with thermocouples), Technisches Messen: 68 (2001), 12, 550 – 557

5 Website address and contact details

A public website is available, where the public can be informed about project news, meetings and events: <http://projects.npl.co.uk/T3D/>

The contact person for questions about the project is Jens Flügge, PTB, jens.fluegge@ptb.de.

6 List of publications

[1] The EMRP project "Thermal design and dimensional drift", J. Flügge, E. Beckert, N. Jennet, T. Maxwell, D. Petit, S. Rudtsch, J. Salgado, M. Schalles, R. Schödel, D. Voigt, M. Voigt, Proceedings 12. EUSPEN International Conference, June 2012, Vol. I, p. 315 (2012)

[2] Metrology to reduce thermal effects and drift in precision engineering, J. Flügge, PTB Mitteilungen, Vol. 122 (2012), Heft 4, p. 71

[3] Untersuchung binärer eutektischer Legierungen für die Kalibrierung von Berührungsthermometern im Raumtemperaturbereich, D. Heyer, B. Polomski, S. Rudtsch, Proceedings Temperature 2013, p. 123-127 (2013)

[4] Dimensional stability validation and sensor calibration with sub-nanometer accuracy, D. Voigt, R.H. Bergmans, Proceedings International Conference on Space Optics 2012, paper ID 123 (2012)

[5] Investigation on the thermal behaviour of an ultra-high precision system used in dimensional metrology, K. Bouderbala, H. Noura, M. Girault, E. Videcoq, J. Salgado, D. Petit Proceedings 14. EUSPEN International Conference, June 2014, Vol. I, p. 305-308 (2014)

[6] Parametric investigation of Linear Quadratic Gaussian and Model Predictive Control approaches for thermal regulation of a high precision geometric measurement machine, E. Videcoq, M. Girault, K. Bouderbala, H. Noura, J. Salgado, D. Petit, Applied Thermal Engineering, Vol. 78, p. 720-730 (2014)

[7] Interferometric characterization of dimensional and thermal stability of materials and joints, H. Lorenz, R. Schödel, Proceedings 14. EUSPEN International Conference, June 2014, Vol. I, p. 301.304 (2014)

[8] Interferometric measurement of dimensional and thermal stability of joints, H. Lorenz, R. Schödel, Proceedings SPIE, Instrumentation, Metrology, and Standards for Nanomanufacturing, Optics and Semiconductors VIII, Vol. 9173, 9173OB (2014)

[9] Picometer resolution heterodyne interferometry for short to medium term dimensional stability measurements, A. van de Nes, D. Voigt, Proceedings 58th IWK, Ilmenau Scientific Colloquium, paper ID 25282 (2014)

[10] Thermometry Fixed-Points Based on Binary Eutectic Alloys, S. Rudtsch, Proceedings 58th IWK, Ilmenau Scientific Colloquium, paper ID 25281 (2014)

[11] Reduction of thermal effects on precise dimensional measurements, M. Schalles, J. Flügge, R. Köning, Proceedings 58th IWK, Ilmenau Scientific Colloquium, submitted, paper ID 25271 (2014)

[12] Absolute interferometric measurement of the dimensional and thermal stability of joining techniques, H. Lorenz, R. Schödel, Proceedings 58th IWK, Ilmenau Scientific Colloquium, submitted, paper ID 25271

- [13] Phase topography-based characterization of thermal effects on materials and joining techniques, H. Lorenz, E. Beckert, R. Schödel, *Applied Optics*, Vol. 54, Issue 8, pp. 2046-2056 (2015)
- [14] A dedicated calibration standard for nanoscale areal surface texture measurements, J. R. Koops, M. van Veghel, A. van de Nes, *Microelectronic Engineering*, Vol. 141, pp 250-255 (2015)
- [15] Stability of thermocouples near room temperature for measurement and control applications in precision engineering, J. Flügge, M. Voigt, *Precision Engineering*, submitted
- [16] A virtual lateral standard for AFM calibration, R. Koops, M. van Veghel, A van de Nes, *Microelectronic Engineering*, Vol. 153, pp 29.36 (2016)
- [17] PCM-shielding of precision measuring equipment by means of latent heat, M. Schalles, T. Fröhlich, J. Flügge, *Precision Engineering*, , Vol. S0141-6359 (15) 00056-2 (2015)
- [18] Thermal investigation on ultra-high precision apparatus for dimensional metrology at the nanometre level of accuracy, K. Bouderbala, H. Noura, M. Girault, E. Videcoq, J. Salgado, *International Journal of Precision Engineering and Manufacturing*, Vol. PP, Issue 99 (2015)
- [19] Good Practice Guide: Traceable calibration of instrumented indentation instruments as a function of temperature, A.S. Maxwell, L. Mera Alvarez, <http://projects.npl.co.uk/T3D/publications.html>
- [20] Good Practice Guide: Measurement of relative length changes in sample up to 50mm with picometre uncertainty over durations up to one week, A. van der Ness, <http://projects.npl.co.uk/T3D/publications.html>.
- [21] Good Practice Guide: Optimising the thermal stability of joints including atleast two examples of exemplarily selected samples, H. Lorenz, <http://projects.npl.co.uk/T3D/publications.html>.
- [22] Good Practice Guide: Thermal modeling of precision engineering equipment, M. Schalles, <http://projects.npl.co.uk/T3D/publications.html>.
- [23] Good Practice Guide: Locating and control cooling devices on thermal sensitive instruments, M. Schalles, <http://projects.npl.co.uk/T3D/publications.html>.
- [24] Good Practice Guide: Developing instruments with minimal thermal sensitivity, M. Schalles, <http://projects.npl.co.uk/T3D/publications.html>.

Furthermore, the following publications are in preparation:

- [25] Pictometer resolution dimensional stability measurements using precision interferometry, A. van de Nes, D. Voigt, H. Lorenz, R. Schödel
- [26] Challenges to achieve isothermal contact between the indenter and the sample in thermal equilibrium, H. Xiaodong, N. Jennet, T. Maxwell, *Philosophical Magazine*